Flocculation as Method for Optimizing Crossflow Microfiltration

Master's thesis
by

Pernille Malthe Rosenkjær

Supervised by assistant professor Morten Lykkegaard Christensen,
Department of Biotechnology, Environmental, and Chemical Engineering,
Aalborg University.

December 2010

AALBORG UNIVERSITY

Flocculation as Method for Optimizing Crossflow Microfiltration
Pernille Malthe Rosenkjær

December 2010
First edition

Printed at Aalborg University
Number of printed copies: 6
Number of pages: 84

Abstract

This master's thesis intends to find a strategy for flocculation as pretreatment to optimize crossflow microfiltration of polystyrene particles suspended in demineralized water. This is done by evaluating some properties of flocculants. The investigated properties include structure, molecular weight, and charge density. The evaluation is done by using three different polymers as flocculant under crossflow microfiltration on a model scale laboratory system. The polymers in question are Zetag 7631 (linear, high molecular weight), polyDADMAC (linear, low molecular weight), and Zetag 7867FS40 (Cross-linked).

The polymer dosage used for the experiments is based on the charge ratio (CR). Three different charge ratios are used for each of the polymers; CR 0.5, CR 1 and CR 2. The critical permeate flux is used as the evaluating factor because it represents the highest flux for which no fouling occurs.

It is concluded that the critical flux increases as the charge ratio increases. Further, using a high molecular weight linear polymer as flocculant gives the best filtration results and highest critical flux.

Danish Summary

Denne kandidatafhandling søger at finde en strategi for flokkulering som forbehandling til optimere af tværstrøms-mikrofiltrering af polystyren partikler suspenderet i demineraliseret vand. Dette gøres ved at evaluere nogle egenskaber for flokkuleringsmidler. De undersøgte egenskaber omfatter struktur, molekylevægt og ladningstæthed. Evalueringen sker ved at bruge tre forskellige polymerer som flokkuleringsmiddel under tværstrøms-mikrofiltrering på et modelskala-laboratorie-system. De anvendte polymerer er Zetag 7631 (lineær, høj molekylærvægt), polyDADMAC (lineær, lav molekylærvægt) og Zetag 7867FS40 (tværbundet).

Den anvendte dosering af polymeren i forsøgene er baseret på ladningsforholdet (CR). Tre forskellige ladningsforhold bliver brugt for hver af de tre polymerer; CR 0.5, CR 1 and CR 2. Den kritiske permeat flux anvendes som evalueringsparameter, fordi den repræsenterer de højeste flux, hvor der ikke sker nogen fouling.

Det konkluderes, at den kritiske permeat flux stiger med et stigende ladningsforhold, og at en lineær polymer med høj molekylvægt som flokkuleringsmiddel giver de bedste filtreringsresultater med den højeste kritiske permeat flux.

Preface

The present master's thesis is submitted in a partial fulfillment of the requirements for obtaining the degree of Master of Science in Chemical Engineering at Aalborg University, the Faculty of Engineering, Science, and Medicine, Department of Biotechnology, Chemistry and Environmental Engineering. The project is prepared under the supervision of assistant professor Morten Lykkegaard Christensen.

The project was started September 1^{st} 2009 and ended December 15^{th} 2010. The thesis is mainly addressed to people with a similar or higher educational level in chemistry or chemical engineering.

A digital copy of the thesis, the experimental data, and the MATLAB scripts used for data processing can be found on the enclosed CD-ROM. All references are made in accordance to the Harvard method, e.g. [Field *et al.* 1995].

I would like to thank laboratory technician Lisbeth Wybrandt for her help during the experimental part of the project and my supervisor Morten Lykkegaard Christensen for his guidance and encouragement. Finally, I will thank my boyfriend Lasse Gillig for helping with the final preparations of the thesis and for his love and support throughout the project.

Pernille Malthe Rosenkjær,

Aalborg, December 2010.

Contents

Chapter 1

Introduction

The industry is interested in having an efficient and fast method for microfiltration at the lowest possible cost. The cost increases as requirements for the pressure and flow velocity increase. One of the bigger problems with microfiltration is the fouling of the membrane, which leads to a slower filtration. To prevent fouling a high crossflow velocity is often applied. However, this is not always enough, and sometimes a pretreatment is necessary.

Previous studies have shown that the permeate flux in crossflow microfiltration can be significantly increased by flocculation. It has been argued that fouling in crossflow filtration in principle is caused by small particles. Flocculation results in an increase in particle sizes and thereby increases the permeate flux [Chellappah *et al.* 2008]. Flocculation is one available pretreatment method, however it is difficult to select the optimum strategy for the flocculation. Most works regarding flocculation to enhance microfiltration have mainly investigated the effect of flocculation on limiting or steady state flux values, not critical permeate flux denoted J_{crit} [Chellappah *et al.* 2008]. The critical flux was first defined in 1995 in the three papers [Field *et al.* 1995], [Howell 1995] and [Bacchin *et al.* 1995]. The main idea behind the J_{crit} is that below it, no fouling occurs. For further details see Section 2.1.4 on page 6.

This thesis will focus on *"Flocculation as Method for Optimizing Crossflow Microfiltration"*. This will be done by looking for a way to select the optimum strategy for a specific flocculation. Polystyrene particles suspended in demineralized water will be used as model suspension for the filtration and flocculation.

Several different polymers are available as flocculant and they differ in charge density, molecular weight, and structure (linear, branched, cross-linked). The influence of the concentration/dosage of flocculant on the ability of the suspension to be filtrated will be investigated. This is done by using three different concentrations. The concentrations are chosen on the basis of the charge ratio between the particles and the flocculant, hence making it possible to compare the result of the filtration using different polymers as flocculants. Further, the effect of the charge density can be determined. The parameter used to evaluate this is the critical flux J_{crit}. The effect of flocculant structure is also investigated. Two different structures are selected; a cross-linked and linear. The effect of the molecular weight on the flocculation and the ability of the filtration is also investigated. This is done by comparing experimental results from a filtrations using a high M_w flocculant (Zetag 7631, Ciba) and a low M_w flocculant (polyDADMAC).

This thesis consist of six chapters and they are arranged according to the standard for scientific papers. Chapter 2 gives a brief introduction to the theory behind crossflow filtration and flocculation. The methods used for the analysis are introduced in Chapter 3 and all the results are shown in Chapter 4. Chapter 5 contains a discussion of the results and finally, Chapter 6 presents some concluding remarks.

Chapter 2

Crossflow Filtration, Fouling and Flocculation

In this chapter the theory necessary to understand the mechanisms of crossflow filtration, fouling and flocculation will be explained. To understand flocculation it is necessary to know something about the movement of particles and which forces make them floc.

2.1 Crossflow Filtration

Crossflow filtration is a filtration where the fluid that is going to be filtrated (Feed) is moving parallel to the membrane, hence crossflow. Because of a pressure gradient drop over the membrane, the fluid flow through the membrane (Permeate). The fluid and particles held back by the membrane (Retentate) can be circulated back to the reactor. The system is sketched in Figure 2.1.

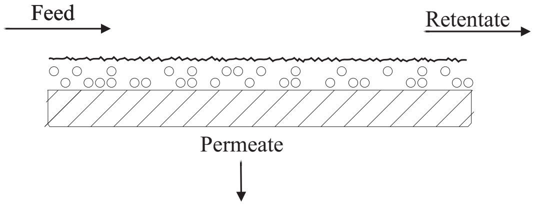

Figure 2.1: Sketch of crossflow filtration, where the permeate, feed and retentate are defined.

The permeate flux through the membrane is symbolized by J and is described by

$$J = \frac{\Delta P}{\eta_d \cdot R_{tot}} \tag{2.1}$$

where ΔP is the pressure drop across the membrane, η_d is the dynamic viscosity and R_{tot} is the total resistance of the flow.

2.1.1 Total Resistance R_{tot}

The total resistance consist of a sum of contributions from different elements: the the resistance from the membrane itself (R_m), the resistance due to blockage of the pores in the membrane (R_{pb}), the resistance due to adsorption to the membrane (R_a), the resistance due to concentration polarization (R_{cp}), and the resistance due to the cake (R_c) [Chellappah *et al.* 2008]. Fouling is characterized by an irreversible decline in the flux [Cheryan 1998], i.e. an addition of resistance that cannot be removed. This is the (R_a) and (R_{pb}). However some would say (R_{cp}) is fouling as well even though it reversible.

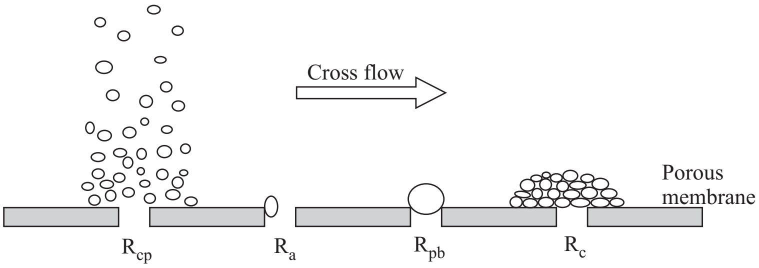

Figure 2.2: Sketch of the types of blockage a crossflow filtration membrane can be subject to. R_{cp} is concentration polarization. R_a is absorption of particles to the membrane. R_{pb} is the blockage of the pore by particles. R_c is the formation of the filter cake of particles on the membrane surface.

Figure 2.2 shows a sketch of the different types of resistance that can occur when crossflow filtrating. First from the left is concentration shown, it is a up-concentration of particles from the bulk phase towards the membrane. Second from the left is the absorption of particles to the membrane shown. Then the blockage of the pore is shown and last the formation of a filter cake of particles is shown. The cake formation is a consequence of concentration polarization near the membrane surface.

2.1.2 Steady State Flux

The steady state flux denoted J_{ss} may at first seem identical to the limiting flux, but that is not the case. The difference between the two is that J_{ss} is dependent on

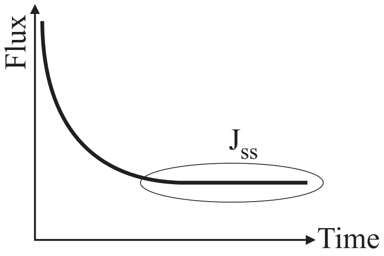

Figure 2.3: Flux at the stationary part is called the steady state flux (J_∞).

the pressure while J_∞ is not. Figure 2.3 shows the flux as a function of time. J_{SS} is indicated by a circle, and it is, as the name indicates, the flux at the steady state of the function. For every pressure there is a J_{SS}. The steady state flux is highly dependent on time, a flux may seem steady over a short period time (minutes) but over a longer duration time (hours) that may not be the case. This all depends on how long it takes the specific suspension to obtain the maximum fouling/blockage of a specific membrane at a specific pressure.

2.1.3 Limiting Flux

The membrane resistance is assumed to be constant, and non-depended on the feed. When filtrating pure water the flux will increase linearly with the trans-membrane pressure. However, this is only the case for pure water. A flux profile for a suspension will look differently because as explained in Section 2.1.1, the membrane resistance is not the total resistance – when filtrating a suspension the particles will add to the total resistance.

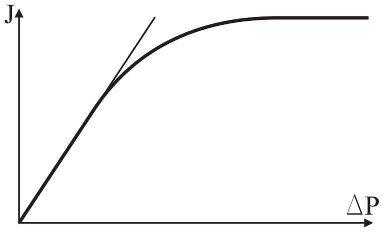

Figure 2.4: The theoretical filtration preformed with pure water and a suspension. The pure water line is the straight one. The curve which bends off and becomes stationary is the suspension line. The flux at the stationary part is called the limiting flux (J_∞).

Figure 2.4 shows the theoretical flux dependency one pressure for pure water and for a suspension. The straight line shows the pure water and the line that bends off shows the suspension. The stationary flux after the bend off is called the limiting flux J_∞. The limiting flux is one of the oldest concepts in crossflow filtration. It represents the maximum stationary flux across the membrane when increasing the transmembrane pressure for a given suspension and it can be varied by changing the crossflow or pretreatment of the feed [Bacchin *et al.* 2006].

2.1.4 Critical Flux

Three different papers published in 1995 defined the J_{crit} for the first time. The three papers are [Field *et al.* 1995], [Howell 1995] and [Bacchin *et al.* 1995]. They each had their own approach for this phenomenon, but the critical flux J_{crit} was essentially defined in two different ways. Either as *the flux at which the transmembrane pressure curve starts to deviate from a straight line* or as *the flux for which the first irreversible fouling appears*. The first definition of the two is developed by [Field *et al.* 1995] and it can be experienced in two different forms, a strong and a weak form.

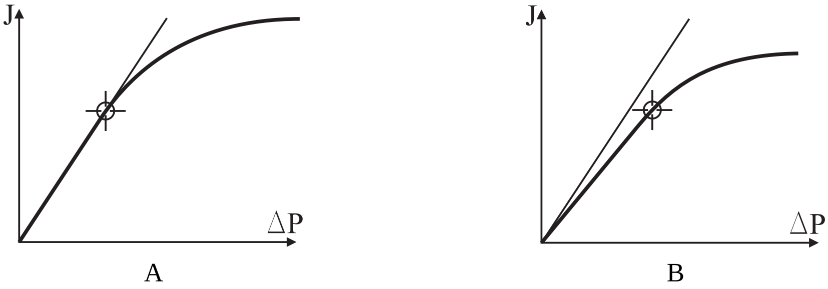

Figure 2.5: Two different definitions of the critical flux A: The strong form B: The weak form.

Figure 2.5 illustrates [Field *et al.* 1995] two forms of critical flux. Figure A shows the strong form, and it is only affected by the resistance derived from the formation of a cake or gel layer. The slope of the straight part is $\frac{1}{\eta_d R_m}$. Figure B shows the weaker form. This form is also affected by the resistance derived from the formation of a cake or gel layer but at the beginning of the experiment there is a quick adsorption to membrane. That is why the straight part of the curve is lower for the weaker form, and the slope is $\frac{1}{\eta_d(R_m+R_a)}$ [Bacchin *et al.* 2006]. When a critical concentration is reached within the membrane boundary layer, this can be defined as the critical flux. It can be viewed as the flux for which the drag force is larger than the thermodynamic forces that keep the particles away from the membrane surface. When the pressure is so high that the flux exceeds the critical flux and particles form a deposit on the membrane, i.e. as gel layer [Aimar & Bacchin 2010].

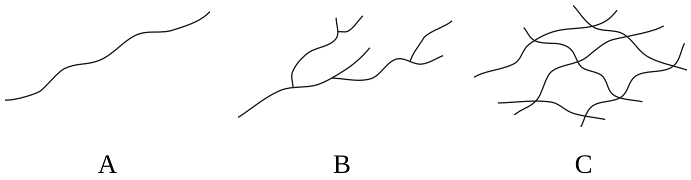

Figure 2.6: The three figures show three different types of polymer structure. A: Linear polymer. B: Branch polymer. C: Cross-linked polymer.

2.2 Polyelectrolyte, Flocculation and Colloids

The fouling can be decreased if the particle size is increased which can be obtained by flocculation. If the particle size increases then it is plausible that J_{crit} can be increased as well. Flocculation is when using a polyelectrolyte to bind particles together in flocs. In solution polymers adopt a random coil configuration. Hence, even though they might be up to $100\,\mu$m long, the net diameter might only be around $1\,\mu$m. When a polyelectrolyte is in solution the charge groups repel each other, and hence the structure have a larger diameter. The salt concentration in the solution influences the structure of the polyelectrolyte. The ions in the solution can screen the charged polyelectrolyte groups from each other, and hence the higher the salt concentration the smaller the diameter of the polymer coil [Gregory 2006]. Flocculants/polyelectrolytes are added in the form of a solution (usually 0.1 - 1 percent) to give the required final concentration in the particle suspension. The final concentration is often in the order of $\mathrm{mg/L}$, thus the polymer solution might be diluted up to a thousand times. To ensure a uniform distribution of polymer in the suspension, an intense mixing is necessary [Gregory 2006]. When the mixing are insufficient, local overdosing can be experienced and other areas can experience lack of polymer. Overdosing can lead to excess adsorption of polymer which may result in destabilization of the particles. This can be a reason why residual fine particles exist and can cause after-flocculation.

Polymers can have different structures; they can be linear, branched or cross-linked in a network, see Figure 2.6. However, nearly all efficient flocculants have a linear structure [Gregory 2006].

2.2.1 Flocculation

When polymers are adsorbed to the surface of the particle they adopt a more restricted conformation than the random coil in the suspension, thus some entropy is lost. For this reason, there must be favorable interactions between the polymer segment and the particle surface. Below, three different types of favorable interactions are described [Christensen *et al.* 2009], [Gregory 2006].

Charge neutralization This happens when a charge flocculent is adsorbed to a particle surface of the opposite charge and the charges neutralize. When the flocculate is small relative to the particle and when the flocculent is evenly distributed on the surface of the particle a homogeneous reduction of the surface charge will take place. This lowers the repulsive electrostatic forces between the particles, and once sufficiently reduced the attractive van der Waals forces will dominate: this will result in a weak aggregation of the particles.

Electrostatic patches This happens when the flocculent is comparable in size to the particle. The polymer gets adsorbed on the surface of the particle in a mosaic pattern. If the distance between the charges on the polymer is less than the distance of the surface charge of the particle, then cationic paths form on an anionic surface. Interactions between such paths and uncovered regions on other particles add an electrostatic contribution to the attractive forces.

Inter-particle bridging This occurs when the flocculent exceeds the size of the particle. Adsorbed polymer chains may reach far into the bulk of the suspension and thus form bridges to other particles.

When polymers are adsorbed they adopt an equilibrium conformation. The dynamics of this process is not yet well understood, but for long-chained polymers it can take several seconds or more to achieve the equilibrium conformation. This may have an imported influence on the kinetics of the flocculation. The mixing causes collision between particles with adsorbed polymer and without, which leads to flocculation. However, the mixing conditions also cause breakage of the flocs [Gregory 2006]. It is generally accepted that the aggregation rate is a balance between floc formation and breakage, and hence the stability of the floc influences the particle size distribution [Jarvis *et al.* 2005].

2.2.2 Colloids Stability

The stability of a floc depends on the strength and number of inter-particle bonds between the particles and polymers. The strength of a floc is considered the energy required to break flocs under tension, compression, or shear stress. Figure 2.7 shows two types of floc breakage: large scale fragmentation under tensile stress and surface erosion under shear stress. The surface erosion causes an increase in the smallest size particles [Jarvis *et al.* 2005]. This is very undesirable because the small particles foul the membrane during filtration.

During crossflow filtration the suspension is in constant movement, thus the flocs are exposed to stress. This can either be a turbulent flow, which causes the particles to whirl or a laminar flow where all particles are moving in straight lines parallel to the walls of the tube.

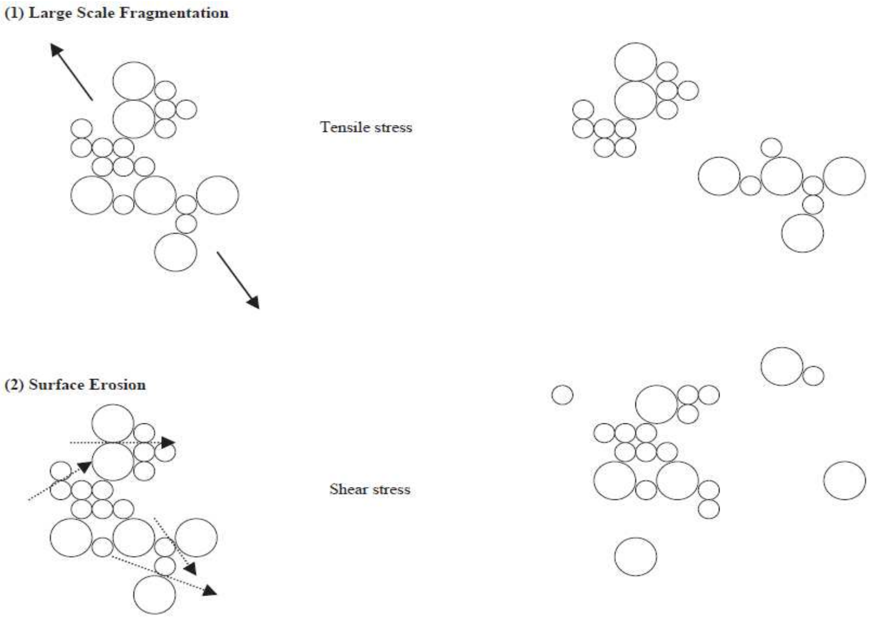

Figure 2.7: Floc breakage cause by tensile stress (large scale fragmentation) and shear stress (surface erosion). This figure is taken from [Jarvis *et al.* 2005].

Reynolds found a dimensionless number that can be used to characterize the flow. The number is therefore called Reynolds number (Re) and can be expressed by

$$Re = \frac{\rho \nu D}{\eta} \tag{2.2}$$

where ρ is the density of the fluid, ν is the average velocity of the fluid, D is the diameter of the pipe/tube and η is the viscosity of the fluid. When Re is lower than 1500 the flow will be laminar and when it exceeds 3000 the flow will be be turbulent. In the range 1500 to 3000 the flow is laminar with a increasing tendency for turbulence [Clement *et al.* 2004].

Chapter 3

Experimental Design

This chapter contains a description of the experiments conducted in this thesis and an explanation for the design of the experimenters. First an experiment overview is given where all conducted experiments are presented. Next, the characterization methods for the polymers and particles are introduced. They are presented in the same order as in the result chapter. Finally, the filtration system on which the experiments are conducted is introduced.

3.1 Experimental Overview

This thesis examines different parameters for optimizing crossflow filtration. The optimum filtration rate is obtained at the critical flux. The higher the critical flux the higher the filtration rate and this is desirable. Polystyrene particles are used in this thesis as model material, an they are flocculated to obtain a higher critical flux. The main question is then how does the polymer and its properties influence the filtration. The properties in question are charge, density, molecular weight, and the structure of the polymer. Three different polymers are tested to answer the question.

Zetag 7631, Ciba A long linear polymer. When mentioned later in the thesis it will be referred to as the "Long polymer" due to its structure.

Zetag 7867FS40, Ciba Poly(acryloxyethyltrimethylammonium chloride-co-acrylamide). When mentioned later in the thesis it will be referred to as the "Cross-linked polymer" due to its structure.

Cat floc (low) Poly(diallyldimethylammonium chloride) has very low molecular weight 35$wt.$% in water. $C_8H_{16}ClN$ is a short linear polymer. The polymer is also known as polyDADMAC. It is from Sigma Aldrich produced in Germany. CAS: 26062-79-3 Batch: 07528 BH. When mentioned later in this thesis it will be referred to as the "Short polymer" due to its structure.

By choosing a long straight polymer and a short straight polymer the result will show if the molecular weight of the polymer makes a difference. But when using two different polymers their charge densities are also different. To overcome this problem the polymer dosage is based on charge ratio (CR) (cf. Equation 3.1). When the dosage is relative to the particle charge present, it also allows determination of the effect of the charge for the flocculation process [Christensen & Keiding 2008].

$$CR = \frac{m_{pol}\sigma_{pol}}{m_{part}\sigma_{part}} \tag{3.1}$$

where σ_{pol} and σ_{part} are the charge densities for the polymer and the particles, and m_{pol} and m_{part} are the masses of the polymer and the particles, respectively. Each of the polymers are tested at three different concentrations. The polymer dose is given by a charge ratio defined by the added cationic polymer charge divided by the anionic charge equivalent for the particle surface.

	CR 0.5	**CR 1**	**CR 2**
Long Polymer	1.6 mg/l	3.2 mg/l	6.3 mg/l
Cross-linked Polymer	4.7 mg/l	9.5 mg/l	19.0 mg/l
Short Polymer	2.2 mg/l	4.4 mg/l	8.9 mg/l

Table 3.1: Concentration equivalent to the charge density for each of the three polymers.

Table 3.1 shows the three different charge ratios and the equivalent concentrations for each of the three polymers. As seen in Table 3.1 the three chosen charge ratios are 0.5, 1, and 2. The concentrations are calculated from Equation 3.1, the charge densities of the polymers are determined in Section 4.1, the charge densities of the particles are found in Section 4.2, and the concentration of the particles which is 1.5 g/l.

	0.4 L/min	**0.6 L/min**
Water	✓	✓
Model Particles	✓	✓
Long polymer	✓	✓
Cross-linked polymer	✓	-
Short polymer	✓	-

Table 3.2: This table shows which experiments are conducted with which of the crossflows. When one of the polymers is checked off it an experiment is conducted for each for the charge ratios.

All the experiments is named after the following convention. The names consist of three parts; the first part tells which polymer is used. The long polymer is called *Long*, the experiments with demineralized water are called *Water*, and the experiments with the model particles are called *Unfloc*. The experiments with the cross-linked polymer are called *Cross* and the ones with the short polymer is called *Short*. The next part of the name is determined by which CR is used and the last part of the name is determined by the crossflow velocity. The name could e.g. be *Long0506* or *Unfloc04*.

3.2 Polymer Characterization

A small amount of flocculant solution is diluted i 100 ml demineralized water. Afterwards a cationic polymer is added in excess (for preforming a back titration). If there is any negative charge present in the solution it will be bound. The remaining of the cationic polymer and positive charge flocculant in the solution will titrated back with a negative charge polymer. Spectrophotometry is used to observe this titration. This is possible when adding a an indicator to the solution. Toluidine blue changes color to red when in a complex with PVS. The change in color can be detected with the spectrophotometry when measuring the absorbance at 620 nm [Kam & Gregory 1999].

Figure 3.1: Color change of the titration when using Toluidine blue as indicator. To the right is the color (blue) in the beginning of the titration and the following beakers contain more and more PVSNa.

Figure 3.1 shows the color change of Toluidine blue when in complex with PVS. The blue color at the left is the starting color of the titration and the pink color on the right is the ending color.

After having preformed a colloid titration the charge density can be calculated from

$$\sigma_{sample} = \frac{N(PVSNa_{blind} - PVSNa_{sample})}{V_{sample}C_{sample}} \tag{3.2}$$

where $\sigma_{sample}[\text{meq}/\text{l}]$ is the charge density of the investigated flocculant and N is the normality of the PVSNa solution $(1.25\,\text{meq}/\text{l})$. V_{sample} is volume of the added flocculant solution, C_{sample} is the concentration of the added flocculant solution, $PVSNa_{blind}$ is the added volume of PVSNa at the endpoint of the titration of the blind sample, and $PVSNa_{sample}$ is the added volume of PVSNa at the endpoint of the titration of the sample.

3.2.1 Analytical Approach

A small amount of a solution of the flocculant (the volumen depend on which polymer and which concentration the solution is) is added to 100 ml of demineralized water while stirring. Then 5 ml of Cat-floc (0.25 g/l solution of poly(diallyl dimethyl ammoniumchloride), low M_w, 20 wt.% in water Sigma Aldrich CAS.no: 26062-79-3 Batch:31597MJ)is added while stirring at 300 rpm. The stirring is continued for 30 sec and then the velocity is decreased to 150 rpm for 60 sec. Next, 2 ml Toluidine blue (0.1 g/l) solution is added. The titration can now begin. The 0.2 g/l PVSNa(Poly(Vinylsulfonic acid, sodiumsalt)25 wt.% in water from Sigma Aldrich Bach:002227ED-505) is added 100 μl at a time. The absorbance is measured at 620 nm. After each measurement the sample is poured back into the beaker. The same procedure is preformed on blind sample of 100 ml of demineralized water.

3.3 Model Particles

The model particles consist of polystyrene and they are approximately spherical and uniform in size. The synthesization of the particles is not a part of this thesis, and they are made a priori. The suspension concentration is therefore determined before use. This is done according to Danish Standard 204. The concentration is determined to 30.54 g/l. Before the suspension is used it is diluted to a concentration of 1.5 g/l. There are two reasons for this; first of all two other reports [Holm 2009] and [Andersen & Nielsen 2007] have suspensions around this concentration experimenting on the exact same system. Secondly, the amount of particles was limited and had to suffice for the entire measurement campaign.

The particles have an negative charge surface, to estimate how negative the surface is, a collide titration is performed and the zeta potential is measured. The particle size distribution is also measured.

3.3.1 Polymeric Titration

The charge density of the styrene particles is essential when choosing the ratio between the polymer flocculant and the particles. The charge density for particles is found by using polymeric titration and the approach is as following: Mix reagent A; a 0.25 g/L poly(diallyl dimethyl ammoniumchloride)solution. 25 mL of demineralized is transferred to 10×50 mL beakers. 50 μL of the styrene suspension is transferred to each of the beakers. The ζ-potential is measured on sample no. 0. Add 10 μL of reagent A to sample no. 1, stir sample and measure the zeta potential. Add 11 μL of reagent A to sample no. 2, stir the sample and measure the ζ-potential etc.

The charge density can be calculated from

$$\sigma_{styren} = \frac{V_{poly} C_{poly} \sigma_{poly}}{V_{sample} C_{sample}} \tag{3.3}$$

where V_{poly} is the volume of added reagent A and C_{poly} is the concentration of poly(diallyl dimethyl ammoniumchloride) in reagent A. σ_{poly} is the charge density of poly(diallyl dimethyl ammoniumchloride) which is 6.19 meq/g [Christensena *et al.* 2009].

Polymeric titration is an analytical approach to obtain the zeta potential for an unknown substance. The principle in this analysis is to measure the ζ-potential (on the ZetaMaster) of the negative particles after adding an known amount of positive polymer to the solution. The polymer in this case is poly(diallyl dimethyl ammoniumchloride). The charge density of the polymer is known and hence the change density of the particles can be determined from the amount of polymer added when the zeta potential of the solution becomes zero.

Zeta Potential Measurement

The zeta potential measurements are preformed on the ZetaMaster (Malvern Instruments). It is done by subjection the suspended particles to an electric field. In a constant electric field, the particles drift at a constant velocity, the electrophoretic mobilities (μ_e). Through the velocity, the Zeta Potential can be determined by using Smoluchowski approximation

$$\zeta = \frac{\eta}{\varepsilon_{dc}} \mu_e \tag{3.4}$$

Where ε_{dc} is the di-electric constant of the solvent and η the viscosity. The determination is done by a software program supplied by the Malvern Instruments.

3.3.2 Particle Size

The ZetaMaster is also used to measure the particle size distribution. This is done by inserting a cuvette with a suspension of particles diluted in demineralized water to an appropriate concentration into the ZetaMaster. It uses dynamic light scattering (DLS) to measure the mobility (the diffusion constant (D)) of the particles. The appropriate concentration is found by adjusting the concentration of the sample so it is detectible by the DLS. The diffusion constant is determined by a autocorrelation function and under the assumption that the particles are spherical the particle diameter can be found by using the Stokes-Einstein equation

$$D = \frac{kT}{3\pi\eta d_p} \tag{3.5}$$

where η is the viscosity, T is the temperature and k is Boltzmans constant [Atkins & De Paula 2006]. If the particles are not spherical, the mean hydrodynamic diameter (d_p) is found. All the data is the average of five individual measurements. The ZetaMaster can measure particles in the range $10\,\mathrm{nm} - 1\,\mu\mathrm{m}$.

3.4 Flocculation

When adding a polymer flocculant to a particle suspension, the intention is to flocculate the particles. The different types and concentrations of polymer used for the experiments is found in Section 3.1. The mixing of the particle suspension and the flocculant is an important factor for the outcome of the flocculation, see Section 2.2. The factor is not investigated in this thesis, but a specific method is selected. The reservoir in the laboratory system has a round bottom and is not well suited for the purpose of the mixing. Thus the mixing is preformed in 2 L Erlenmeyer flask before it is poured into the reservoir. The polymer solution is transferred by pipette and slowly dripped into the suspension while it is stirred rapidly by a magnet. The rapid stirring continues for 5 min before it is slowed down and stirred slowly for another 5 min before it is poured into the reservoir.

The measurement of the size distribution is a method of documenting that this actually happens. It can also be used to se if there is any differs in the size when adding different polymer dosage to the suspension. The un-flocculated particle size distribution is measured on the ZetaMaster but the sizes of the flocculated particles are to big to be measured by the same instrument(they are larger than $1\,\mu$m). Therefore, they are measured on the Microtrac(Leeds and Northrup model 7997) which is able to measure above $7\,\mu$m. The Mcrotrac also uses DLS for determining the size of the particles. The largest difference between the two instruments is the fact that the zetaMater measures on a stationary sample while the Microtrac measures on a moving sample and the sample volume is much larger when using the Microtrac. The fact that the sample is moving might influence the size of the flocs, because the gradients in the flow velocity might tear them apart. The results from the Microtrac are averaged over two measurements each taken over a duration time of 20 sec.

3.5 Micro Filtration

The system on which the experiments are carried out is displayed in Figure 3.2. The system has a main circuit where the fluid is retained by the membrane and circulates. This main circuit has a reservoir in which the fluid is stirred, a pump to get the fluid flowing, a pressure gauge the monitor the pressure, a flow gauge to monitor the flow velocity, and a house that holds the membrane in place.

The reservoir holds a maximum of 4 L and the experiments are carried out over a

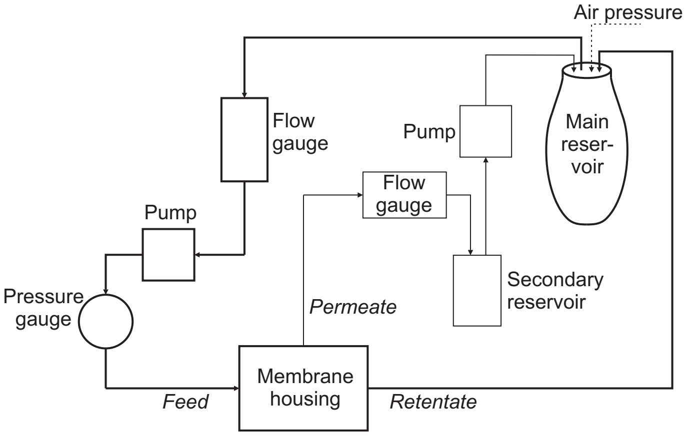

Figure 3.2: The system the experiments is carry out on. The main circuite is make by the thicker black line. The arrows makes the direction the fluid flow. Besides the main circuite their is a flow gauge for measuring the permeate flow, an pump that pumps the permeate back to the main circuite and an air inlet, which is used to controlled the pressure in the system.

time period of 5 to 6 hours. Therefore, the reservoir would be drained before the end of the experiment if the permeate was not reintroduced into the reservoir. This is the reason for the pump outside the main circuit. The available pump is not able to pump the permeate back quickly enough when the pressure is at the highest. For this reason a secondary similar pump is used for last couple of pressure steps, hence doubling the speed of the back flow. Sometimes the pumps stop for no reason and to restart them, they were shut off for a short period of time.

3.5.1 Calibration of Pressure Gauge

The new pressure gauge has a range of 0 – 4 bar and was installed in the system setup. Before being used the gauge was calibred/fitted to the software used to sample the data. The calibration was conducted by adding a known pressure to the gauge and then recording the corresponding bit number. A trendline was fitted to the data and an equation the the calibration was found as shown in Figure 3.3. The equation was written into the data logging program, which is then able to convert the bit number it receives from the PMD to a pressure.

3.5.2 Calibration of Flow Gauge

The flow gauge had already been calibrated from previous projects. However, after the first few experiments were conducted there seemed to be discrepancies between the flow measured by the flow gauge and the capacity of the pump used to pump the permate back into the system. Therefore an additional calibration of

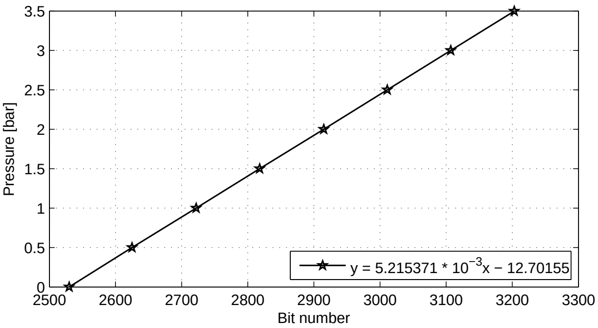

Figure 3.3: The trendline added is fitted with A an R^2 value of 0.999.

the flow gauge was conducted.

To ensure the calibration was performed for the appropriate flow range, the water flow through the membrane at the pressures used in the experiments was used for the calibration. The flow was measured by the flow gauge as usual and at the same time the cumulated weight of the water that had passed through the flow gauge was measured by a scale connected to a data acquisition computer. By differentiating the signal for the cumulated weight with respect to time, the flow measured by the scale is derived. The resulting time series of flow is compared to the signal from the flow gauge in Figure 3.4.

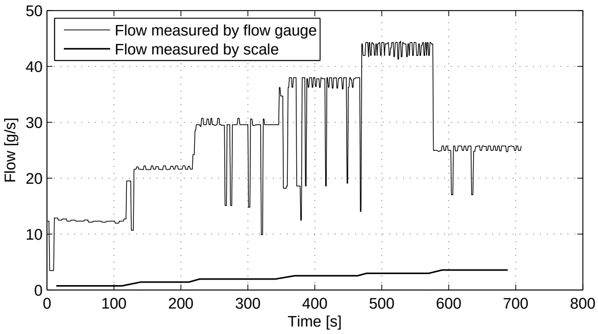

Figure 3.4: Flow measured by flow gauge compared to the same flow measured by a scale. The original calibration of the flow gauge is used here.

The pressure is increased throughout the experiment, and hence the flow becomes higher and higher. This is also reflected in the time series measured by the scale, but the data from the flow gauge shows a drop at the last step. The flow drop indicates the maximum flow velocity that the flow gauge is able to measure.

In each step the mean value is computed for both the scale and the flow gauge,

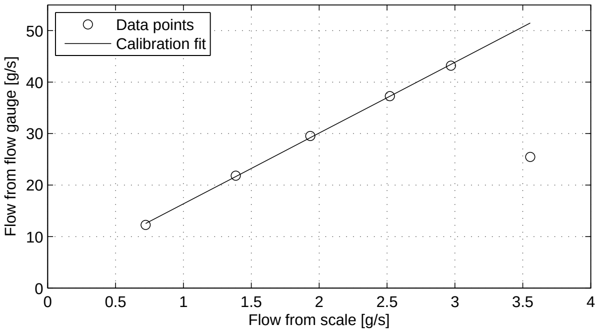

Figure 3.5: Compartment of data points

which yields six five data points, since the last point is discarded due to the maximum capacity of the flow gauge. A line is fitted to the data as shown in Figure 3.5. From the fitted line it is seen that the flow from the flow gauge should be multiplied with a scale (0.0202) and have an offset (-0.0527) added to give the correct flow. In Figure 3.6 the two data sets are shown after the flow gauge has been re-calibrated.

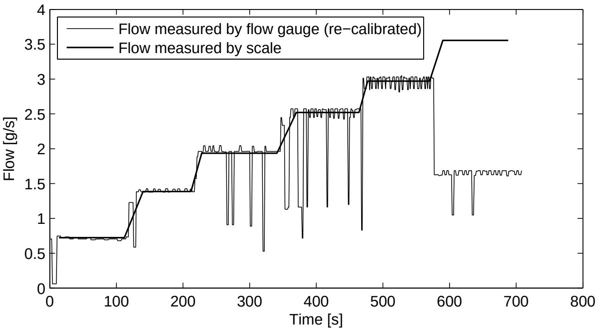

Figure 3.6: Flow measured by flow gauge compared to the same flow measured by a scale. The new calibration of the flow gauge is used here.

3.5.3 Membrane Housing

Two pieces of membrane are housed in the membrane housing, which consists of two identical plates of plastic hold together by six screws. The membrane surfaces are facing away from each other and against the two plates. They are separated by two pieces of porous material which have a very low resistance to the permeate passing through it. The membrane housing is shown in Figure 3.7. Although it seems like the flow is passing in the four cavities the particles are spread evenly all over the membrane surface after a filtration. Hence, when cal-

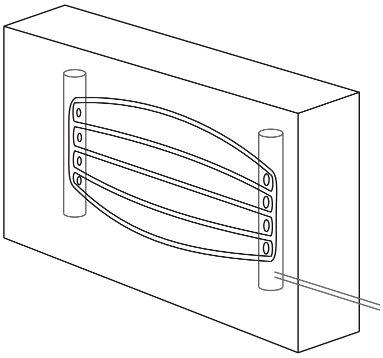

Figure 3.7: Membrane housing.

culating the membrane surface used the entire area of the elliptical membrane is measured. The membrane used in all the experiments is floupolymer membrane (FSM 0.45PP) from Alfa laval. A new membrane is used to each of the experiments, and before use it is cleaned according to Laval [2006]. The cleaning process consist of three steps: first the flush through with demineralized water for 10 min. Second the system is flushed with 0.1% NaOH (J.T.Baker CAS No.: 1310-73-2. Bath;0627503023)solution for 10 min. Last the system is flushed with demineralized water for 10 min before use.

3.5.4 Experimental Approach

In experiments with crossflow filtration either the pressure or the permeate flux is kept constant. The main focus area in this thesis is the critical flux, and one of the main methods for determining the critical flux is by pressure stepping [Bacchin *et al.* 2006]. Under this approach the pressure is increased and decreased following a predetermined pressure profile and the corresponding permeate flux is measured.

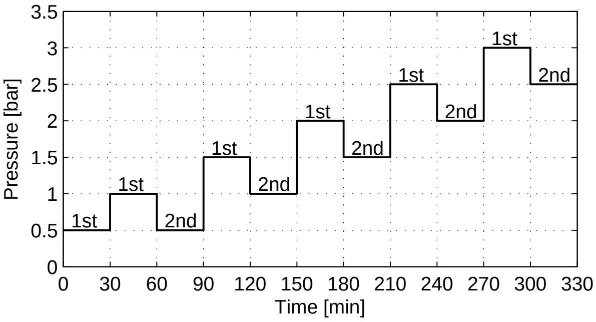

Figure 3.8: Pressure profile all the experiments follows.

Figure 3.8 shows the pressure profile used in all the experiments preformed. The profile is adopted from [Espinasse *et al.* 2002], though it is not the exact same pressure profile. The difference is that [Espinasse *et al.* 2002] has an additional down stepping sequence after the profile shown in the figure.

The profile in Figure 3.8 is chosen because it is possible to analyze the reversibility of the fouling for each of the pressure steps. This makes the determination of the critical flux fairly accurate [Bacchin *et al.* 2006]. The reversibility of the clogging of the membrane can be analyzed by comparing the two steps at the same pressure; if the same permate flux is reached the clogging is reversible [Espinasse *et al.* 2002]. The duration time for each step is important because the flux may appear steady during a short period of time, but it might not be over a longer period of time [Bacchin *et al.* 2006]. Each pressure step for the experiments preformed is 30 min because it is a sufficiently long period of time to get an indication of stability in the permate flux, and further it is short enough so an experiment can be preformed in one day.

Chapter 4

Experimental Results

This chapter presents and discusses all the experimental data obtained in this thesis. First, the polymer and particle characterizations are shown and finally the the flux data from the step function experiment is treated.

4.1 Polymer Characterization

This section contains the results from the colloid titrations described in Section 3.2 of the three different polymers. Further, the charge density (σ_{poly}) is calculated for each of them. The three polymers are presented one at the time.

As stated in the introduction the size of the particles influences their ability to be filtrated. This is a reason for measuring the size distribution of the styrene particles after they have been flocculated. A sample of 20 mL is prepared for this experiment. The small sample is treated the same way as the sample used for the filtration. This means that the sample is heavily stirred for 5 minutes after adding the the flocculant one drop at a the time. Then, the suspension is stirred additionally for 5 minutes at a lower velocity. After the preparation, the size of the particles in the sample is measured by the Microtrac.

4.1.1 Long Polymer

Figure 4.1 displays the result of the titration of the long polymer. Two lines are fitted to the data set. The intersection of the lines marks the high endpoint of the titration. The vertical lines are added to make it easier to read the value of the endpoint. According to equation (3.2) the endpoints are respectively called $PVSNa_{blind}$ and $PVSNa_{sample}$, for the water and flocculant. All the variables of

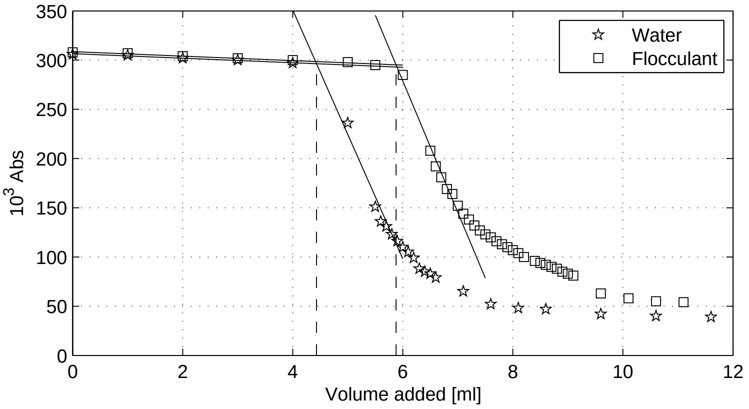

Figure 4.1: Absorbance as a function of added PVSNa for the titration of the flocculant (Zetag 7631) and demineralized water. The endpoint for each of the titrations is found by the intersection of two fitted lines and is indicated by a vertical line.

equation (3.2) are now known. The charge density of the flocculant is

$$\sigma_{sample} = \frac{1.25(4.43 \cdot 10^{-3} - 5.87 \cdot 10^{-3})}{30 \cdot 10^{-6} \cdot 10} = 6.0\,\mathrm{meq/g}$$

This result is used to calculate the amount of polymer added to the suspension of particles for each of the experiments. The amounts can be found in Table 3.1 on page 12. The floc sizes are measured for each of the experiments and the results for the long polymer can be seen in Figure 4.2. The figure shows that CR 1 and

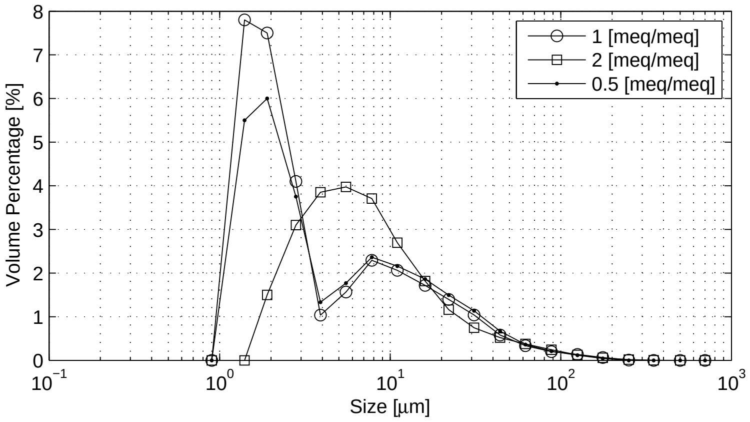

Figure 4.2: Size distributions of particles flocculated by the long polymer.

CR 0.5 have essentially the same distribution, though with the little difference that

CR 1 has a small increase in size. For CR 2 the distribution is clearly different from the other two; it only has one peak. Further, the particle size is clearly larger.

4.1.2 Cross-linked polymer

The charge density of the cross-linked polymer is determined using the procedure in Section 3.2. The structure of a cross-linked polymer makes it difficult to determined the charge density because maybe not all charges are accessible. However, no special considerations are made compared to the two straight polymers.

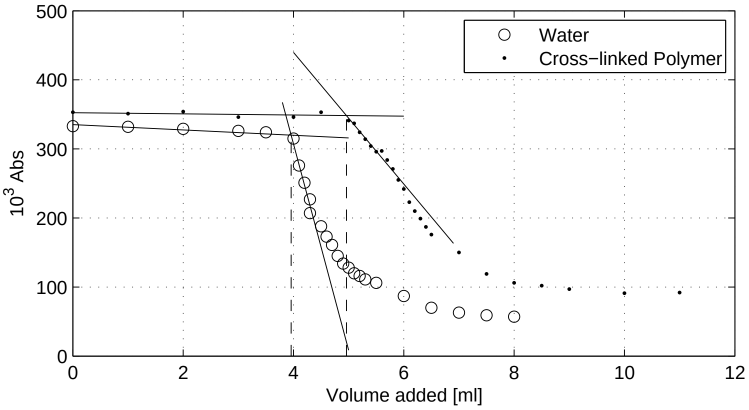

Figure 4.3: Absorbance as a function of added PVSNa for the titration of the flocculant (Zetag 7867FS40) and demineralized water. The endpoint for each of the titrations is found by the intersection of two fitted lines and is indicated by a vertical line.

Figure 4.3 shows two sets of data. One is the colloid titration of water and the other is the colloid titration of the cross-linked polymer. The high endpoint of each titration are marked by two straight lines crossing. Two vertical lines are added to ease the reading position of the line intersections. Based on the found result and Equation 3.2 the charge density is determined

$$\sigma_{sample} = \frac{1.25(3.96 \cdot 10^{-3} - 4.96 \cdot 10^{-3})}{0.1 \cdot 1 \cdot 10^{-3}} = 12.5\,\mathrm{meq/g}$$

The result seems high unlikely because it exceeds the maximum charge density for this polymer. Christensen *et al.* [2009] found the exact same polymer to have a charge density of 1.96 meq/g which seems plausible. Thus, 1.96 meq/g is used for the calculations of the charge ratios/polymer dosage for this flocculant, which is shown in Table 3.1 on page 12.

Figure 4.4 depicts a clear difference between functions for the three CR. It is fairly surprising that the CR 2 (the one with the most polymer flocculant) has the largest

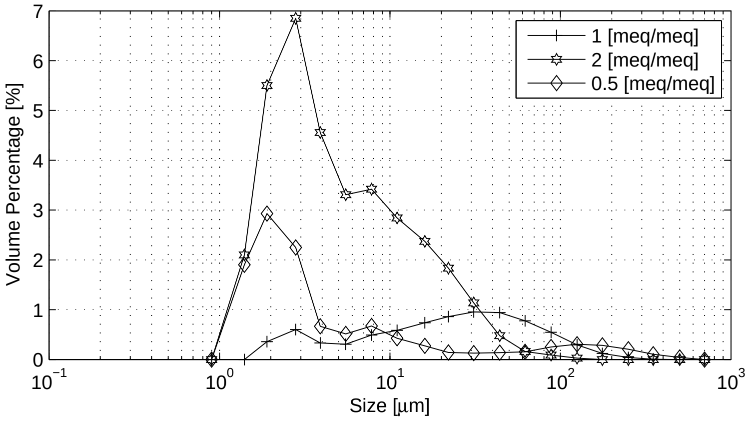

Figure 4.4: Size distributions for particles flocculated by the cross-linked polymer. All three CR are shown.

fraction of small particles while the CR 1 has the smallest fraction. The size ranges measured by the Microtrac is $10^0\,\mu$m to $10^3\,\mu$m. The two CR 0.5 and 1 have particles distributed throughout the range while the CR 2 have no particles with a size bigger than $10^2\,\mu$m.

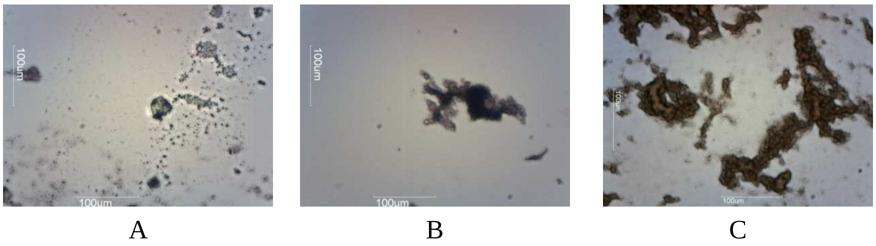

A B C

Figure 4.5: The three pictures are taken by a microscope with a 40x lens and show flocs of the styrene particles and the cross-linked polymer. A: CR 0.5 B: CR 1 C: CR 2

Figure 4.5 shows pictures of the flocs for the experiments Cross0504, Cross104, and Cross204. All three pictures have a size bar of $100\,\mu$m and the structures of the flocs can be seen. Picture A shows the CR 0.5, B the CR 1 and C the CR 2. It is seen in all the pictures that the floc are not dense and certainly not spherical. The smallest of the particles can not be seen in these pictures, and hence they do not reflect the particle size distributaries. This is also the reason that there is only picture for the cross-linked polymer, because this polymer have the largest particles sizes, although Figure 4.9 shows differently. This can be because the strength of the floc is insufficient to sustain the integrity in the Microtrac. This could indicate that the long polymer have the strongest flocs or that the Microtac is not able to measure that large flocs.

4.1.3 Short Polymer

The charge density of the short polymer is also found by colloid titration. Figure 4.6 shows the result of the titrating. The two functions display the titration of water with the polymer used to absorb any negative charge (though it is not necessary) and the titration of the same plus the short polymer sample. The intersection of the two lines fitted to each of the data sets indicate the high endpoint of the titration which is used for the calculation of the charge density. As previous, the vertical lines are included for easier reading of the endpoint values. The charge density is

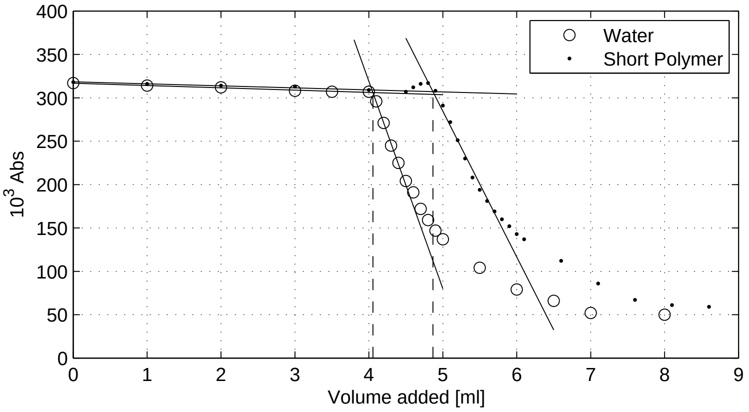

Figure 4.6: Absorbance as a function of added PVSNa for the titration of the flocculant (polyDADMAC) and demineralized water. The endpoint of each of the titrations is found by the intersection of two fitted lines and is indicated by a vertical line.

$$\sigma_{sample} = \frac{1.25(4.05 \cdot 10^{-3} - 4.87 \cdot 10^{-3})}{70 \cdot 10^{-6} \cdot 3.5} = 4.18\,\mathrm{meq/g}$$

From the calculation it can be seen that the charge density of the short polymer is 4.18 meq/L which seems like a fair value. It used in the calculation of how much polymer to use for the flocculation when the three charge ratios are applied. The results can be seen in Table 3.1 on page 12.

The result of the polymeric titration is displayed in Figure 4.7. It shows the zeta potential as a function of added volume [μL] of positive polymer (polyDADMAC).

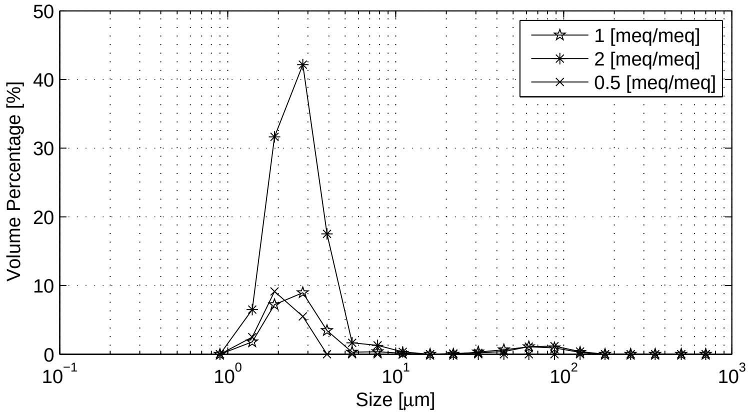

Figure 4.7: Size distribution of flocs for the three CR's for polyDADMAC.

4.2 Model Particles

The charge density of the particles is found by polymeric titration, see Section 3.3.1. Figure 4.8 shows the zeta potential as function of volume of the added positive charge polymer. For each sample five measurements are made, and the error bars in the figure show the maximum and minimum value measured. The figure shows

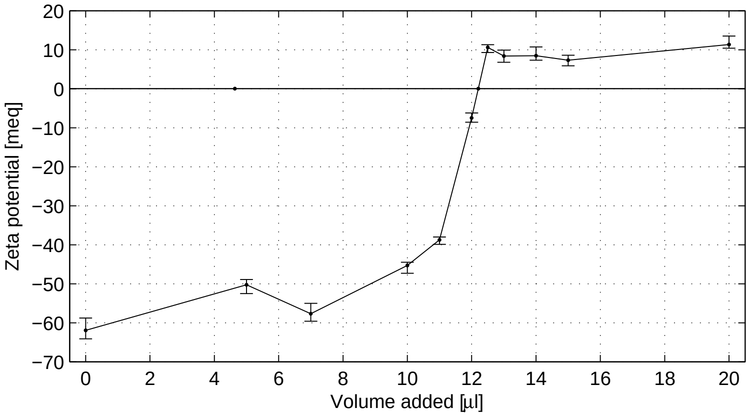

Figure 4.8: Charge density of styrene particles determined by polymeric titration and measurement of the zeta potential on the ZetaMaster. The zeta potential of the particles is shown as a function of added polyDADMAC.

the interception with the x-axis is 12.2 μl. All that is needed to calculate the charge density, with Equation (3.3) is the concentration of the styrene particle solution, which is $C_{sample} = 30.54\,\mathrm{g/l}$

$$\sigma_{styren} = \frac{12.2 \cdot 10^{-6} \cdot 0.25 \cdot 6.19}{50 \cdot 10^{-6} \cdot 30.54} = 0.0124\,\mathrm{meq/g}$$

The charge density of the particles is found to be $0.0124\,\mathrm{meq/g}$, and this value is used for the calculations of Table 3.1 on page 12.

The sizes of the styrene particles are mostly too small to be measured by the Microtrac on which the flocs size distributions are measured. Hence, the particles size are measured on the ZetaMaster.

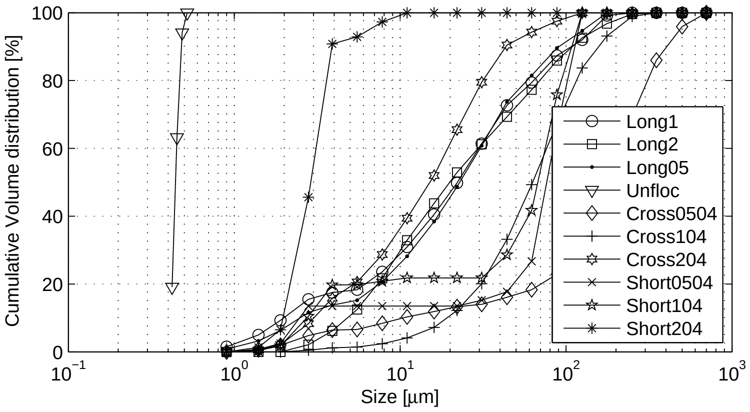

Figure 4.9: The cumulative size distribution of the styrene model particles and all the floc sizes for the different CR's and flocculants.

Figure 4.9 shows the size distributions for the styrene particles and all the flocs. The most important thing to note on this figure is that all the flocs are in the micrometer range while the model particles are in the nanometer range. Also the model particles are quite uniform while the flocs are not. The narrow size range the particles are distributed over is part of the reason they were chosen for model particles.

4.3 Micro filtration

The results from all experiments with micro filtration are presented by showing a plot of the flux vs. time and a graph showing both the pressure vs. time and the resistance vs. time. The resistance is not the exact description of the data shown; more precisely it is the resistance multiplied with the viscosity. The viscosity is the same for all the experiments, and thus it is disregarded throughout the rest of the thesis.

The data shown has been processed to remove spurious data points and it has been averaged with a running average over 20 time steps. The process from the raw data to the data presented in this section is described in details in Appendix A.

The sampled data is calibrated according to Section 3.5.2 except for the data from the un-flocculated particles. They are not calibrated because the flux becomes negative with the determined expression for the calibration. This indicates that the calibration coefficients are not totally correct; during the experiment a flow through the membrane was observed, and therefore the measured negative flux is not trusted.

4.3.1 Water

Two experiments are carried out with demineralized water. The difference between them is the crossflow velocity of respectively 0.4 L/min and 0.6 L/min. First up is Figure 4.10 and it shows flux vs. time for Water04 (see page 13 for a definition of experiment names).

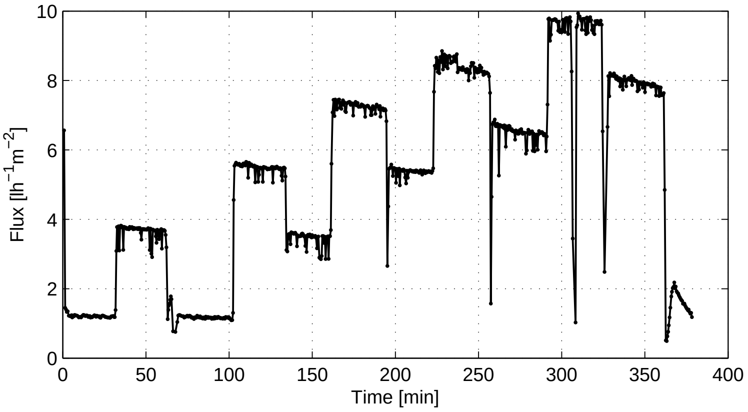

Figure 4.10: Flux vs. time plot for the filtration preformed with demineralize water at crossflow velocity 0.4 L/min.

Figure 4.10 depicts a clear change in the flux approximate every half hour. This is due to the pressure model used. The pressure model is to be like Figure 3.8, but it is not a complete replica – there are minor differences. This applies to all of the experiments. The accurate pressure model for this experiment can be seen in Figure 4.11 which presents time series of both the pressure and the resistance. The resistance represents R_m and is uniform throughout the experiment as expected.

At the step when the pressure is 3 bar, a sudden pressure drop is can be identified in the middle of the step. This is a result of having to stop the experiment briefly. The container used for collecting the permeate was overflowing and consequently

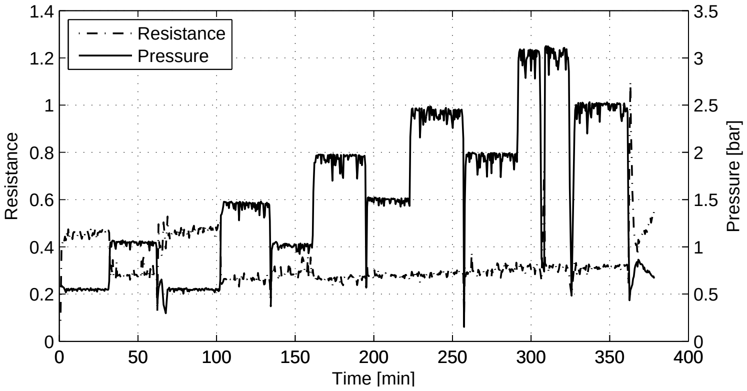

Figure 4.11: Resistance development over time for the filtration preformed with water and a flow of $0.4\,\mathrm{L/min}$.

the system was nearly emptied for water. The water was pumped back and the experiment was restarted. Data was collected during the entire process.

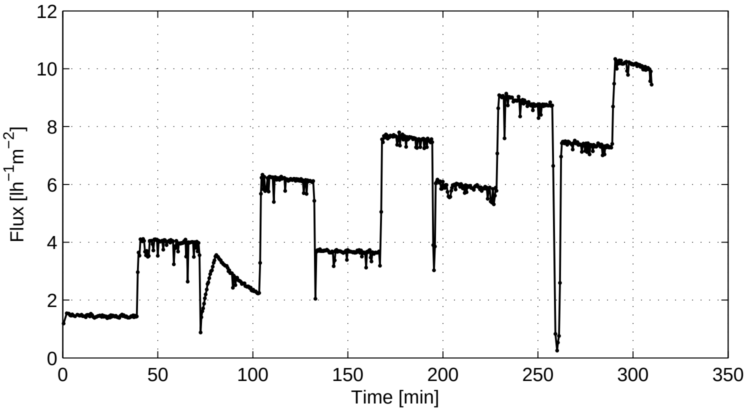

Figure 4.12: Resistance development over time for the filtration preformed with water and a flow of $0.6\,\mathrm{L/min}$.

Figure 4.12 shows the flux vs. time graph for Water06. All the steps are relative horizontal except for the step where the pressure is $0.5\,\mathrm{bar}$ the second time. This can be explained if looking at Figure 4.13 which shows the corresponding time series of pressure. It is seen that in the concerned step the pressure shows the same behavior as the flux. The reason for the strange behavior in pressure is unknown. Some pressure drops can be seen when stepping down. During the process of decreasing the pressure over the membrane, a valve to the main reservoir is opened which causes the pressure in the main reservoir to drop to close to atmospheric

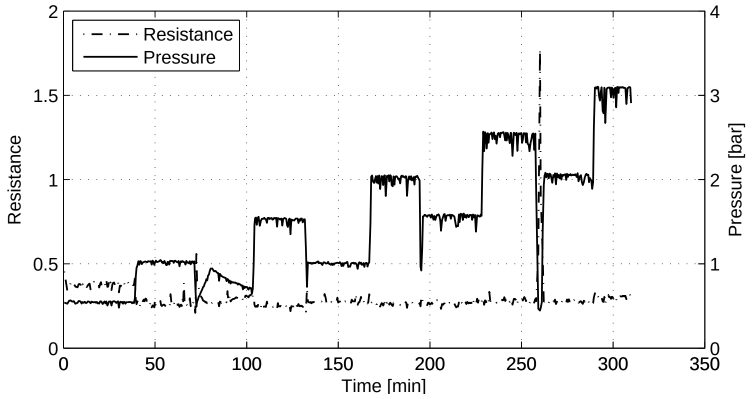

Figure 4.13: Filtration preformed with water and a flow of 0.6 L/min.

level. Next, the pressure is increased again to the desired level by the air pump.

Figure 4.13 also shows the resistance development over time. Like in Figure 4.11 the resistance shows R_m and it is also quite stationary throughout the experiment. A linear regression is fitted to each of the data series for the two water experiments.

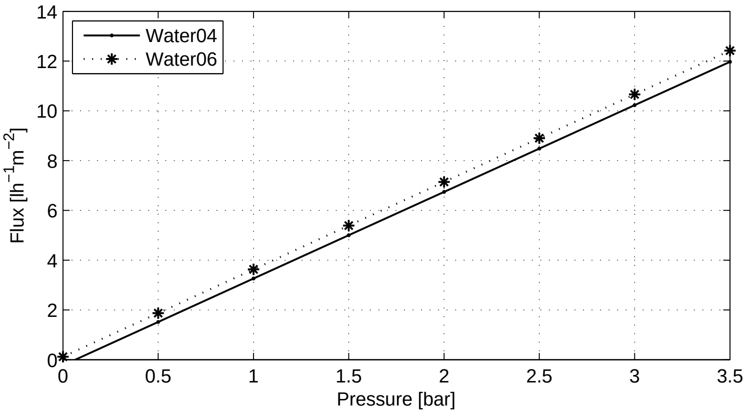

Figure 4.14: Linear fits for the each of the two data sets for water at the two different flows. The R^2 value is 0.96 and 0.97 for respectively water with the crossflow 0.4 L/min and 0.6 L/min.

They are displayed in Figure 4.14. The graph shows that the two lines are quite parallel and that the higher flow give a small increase in flux though the membrane. The two lines are expected to be similar because they are only affected by R_m.

4.3.2 Un-flocculated Particles

This section presents the results from the two experiments where no flocculant were added to the styrene particles. The two experiments will be called Unfloc04 and Unfloc06. First, Figure 4.15 shows the time series of flux for Unfloc04. The graph shows that all the steps are not horizontal and J_{ss} is not reached at any of the steps. This means that J_{crit} is below the flux found using 0.5 bar pressure. After the first 2 bar pressure step the flux decreases rather than increases or become stationary like theory dictates (cf. Section 2.1).

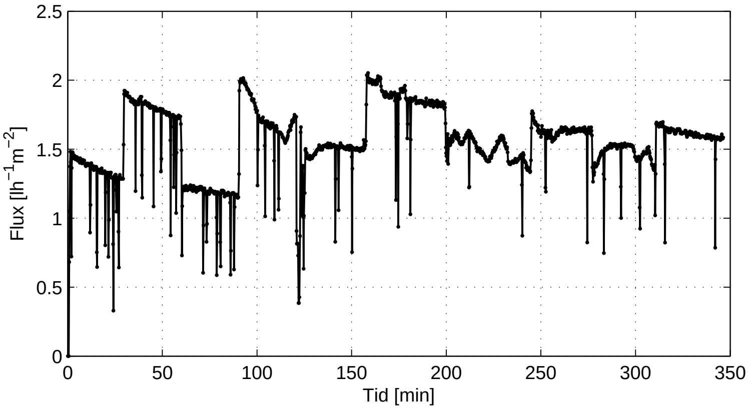

Figure 4.15: Filtration preformed with the model particles and a flow of 0.4 L/min . The data set from this experiment is not calibrated unlike the rest of the data sets.

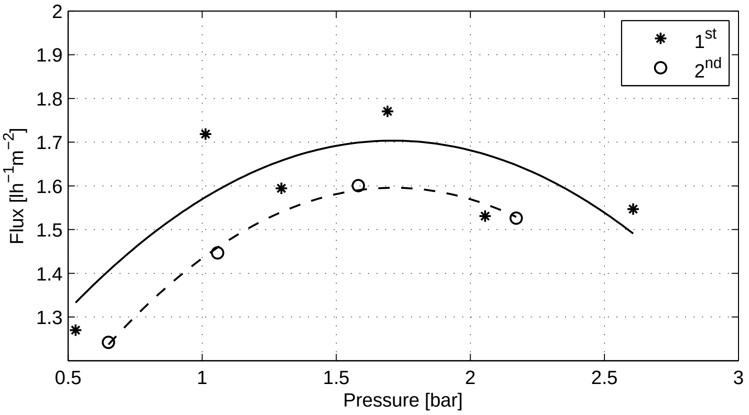

Figure 4.16: Average flux and pressure for each step in the Unfloc04 experiment. The curves are second degree polynomials fitted to the data points. The notation 1^{st} and 2^{nd} is defined in Figure 3.8. The polynomials are fitted with R^2 of respectively 0.64 and 0.99.

Figure 4.16 shows flux dependence of the pressure, using an average value to represent each of the steps. The curves in the figure are second degree polynomials. They are fitted to values representing the 1^{st} and 2^{nd} time a pressure is reached. If below J_{crit} the two curves should be similar. The fact that they are not only reinforces the point made from Figure 4.15 that J_{crit} is below the flux found using 0.5 bar pressure. The fact that the points are not positioned precisely at the pressures they should represent is caused by the pressure being hard to set accurately.

Figure 4.17 shows the pressure profile and the resistance development over time. There is nothing unusually with the pressure profile. The mean point to make about the resistance development is the high spike in the beginning. This could be caused by an adsorption, hence the J_{crit} follows Field *et al.* [1995] weaker from, cf. Section 2.1.

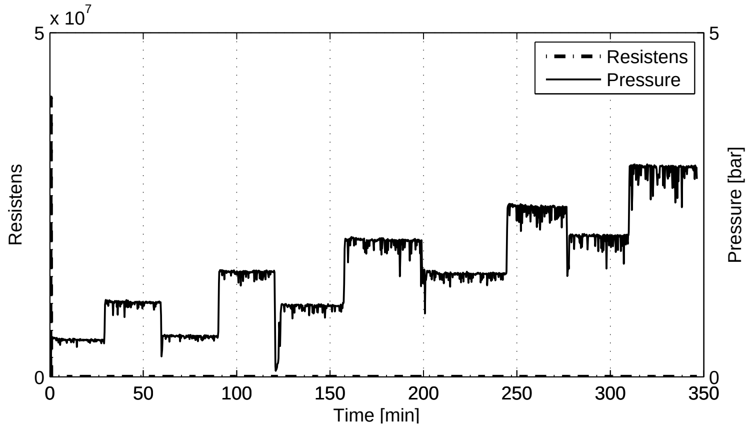

Figure 4.17: Resistance development over time for the filtration preformed with the model particles and a flow of 0.4L/min .

Figure 4.18 shows the flux vs. time for Unfloc06. All the first steps seem to have a slope less than zero while the second steps seems to be horizontal. The absolute value of the slops of the first steps decreases as the pressure increases. The steps with corresponding pressures between 0.5 bar and 2 bar does not reach J_{ss} while it is unclear if last two steps reaches J_{ss}. This indicates that no fouling occurs when a pressure is reached for the second time. Because the first step has a slope, J_{crit} is assumed to be a flux below the one found when using a pressure of 0.5 bar

Figure 4.19 shows the correlation between flux and pressure for Unfloc06. Two second degree polynomials that are fitted to respectively average values representing all the 1^{st} times and all the 2^{nd} times a pressure is reached. Although using a second degree polynomial the lines are fairly straight. There are quite similar; there are small differences between them in the beginning and they cross at the end. It does not seem like the curve bend off indicating the critical flux, but according

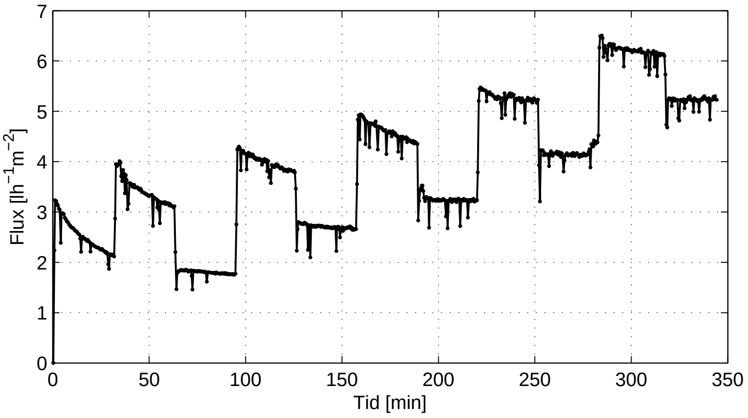

Figure 4.18: Filtration preformed with model particles and a flow of 0.6 L/min

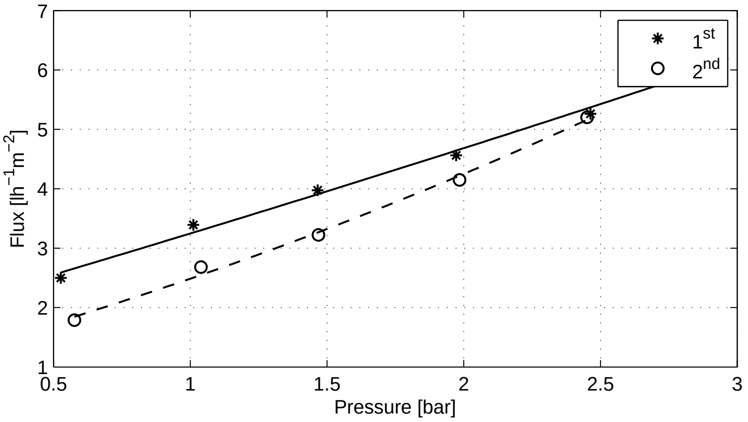

Figure 4.19: Average flux and pressure for each step in the Unfloc06 experiment. The curves are second degree polynomials fitted to the data points. The notation 1^{st} and 2^{nd} is defined in Figure 3.8. Both polynomials are fitted with R^2 of 0.99.

to the step figure 4.18 all the data should be above the critical flux. It could be possible that the curvature should be low and the point where they cross is near J_∞ and they will start to be horizontal. Figure 4.20 shows the pressure profile for Unfloc06 and the resistance development over time. It looks like the previous graph, cf. Figure 4.17. It has the large spike in the beginning, and as before this could indicate Field *et al.*'s [1995] weaker J_{crit}.

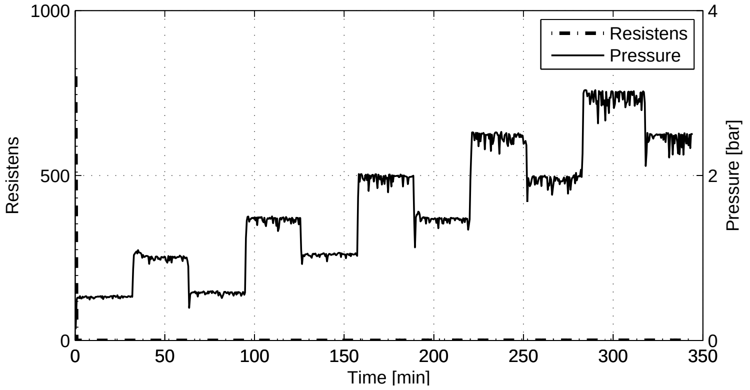

Figure 4.20: Resistance development over time for the filtration preformed with model particles and a flow of 0.6 L/min.

4.3.3 Long Polymer

In this section all the results from the experiments carried out with the long polymer used as the flocculant are presented. The section is divided into three subsections after the concentration ratio used.

CR 0.5

Figure 4.21 shows the flux vs. time for Long0504. All of the steps seem to have

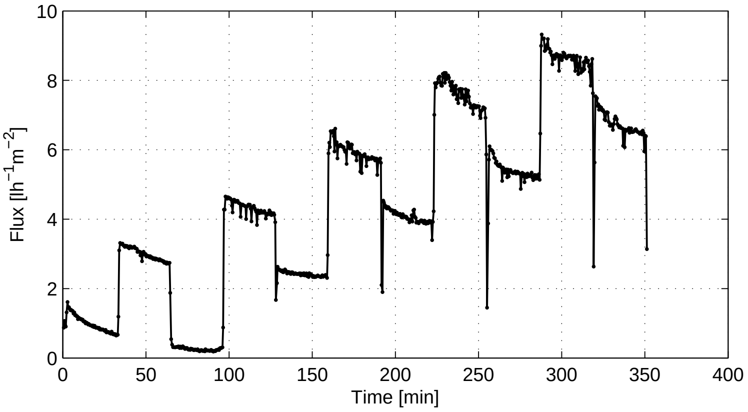

Figure 4.21: Filtration with model particles flocculated (ratio 0.5) and a flow of 0.4 L/min.

a slope, indicting that the J_{crit} is below the detection limit for these experiments. Also indicated is that step two a the individual pressure do not regain the same height of flux as step one. It is difficult to assess if any of the steps that have a slope reaches J_{ss}. Figure 4.22 shows the correlation between flux and pressure for

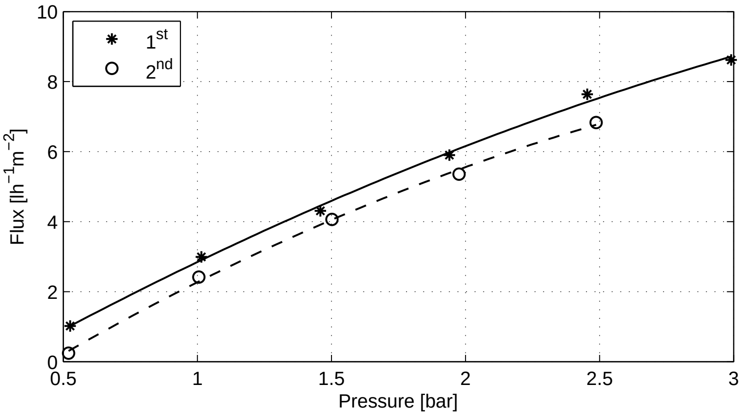

Figure 4.22: Average flux and pressure for each step in the Long0504 experiment. The curves are second degree polynomials fitted to the data points. The notation 1^{st} and 2^{nd} is defined in Figure 3.8. Both polynomials are fitted with R^2 of 0.99.

Long0504. Two second degree polynomials are fitted to the average values for the pressure steps: one representant for each of the 1^{st} and one representant for each of 2^{nd} pressure steps. The curves fit the data quite well, with R^2 of 0.99 for the both of them. There is only a little distance between the two curves, but it still enough to reinforce the assessment that J_{crit} is below the detectable limited for these experiments.

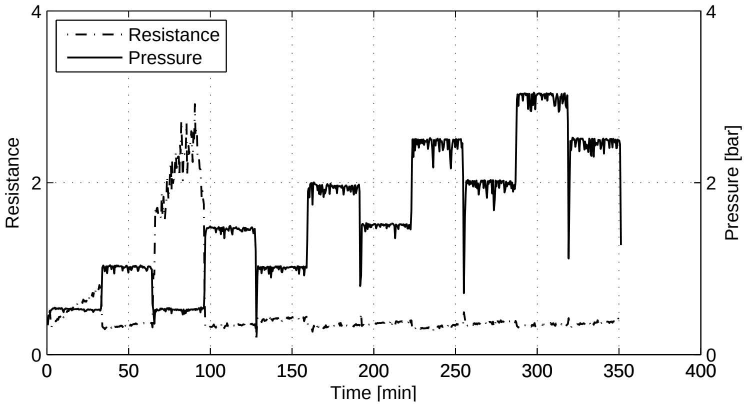

Figure 4.23: Resistance development over time and the pressure over time for the filtration of the long polymer CR 05 and a flow of 0.4 L/min .

Figure 4.23 shows the pressure profile for Long0504 and the resistance development over time. There is nothing usually about the pressure profile. However, an interesting point should be noted about the resistance development. Step one has an increasing resistance, which corresponds well with Figure 4.21 where the flux decreases for the same step. Another thing is the very high resistance (compared to the rest of the experiment) at the second step at 0.5 bar. The reason for this is unknown. The rest of the resistance is quite uniform.

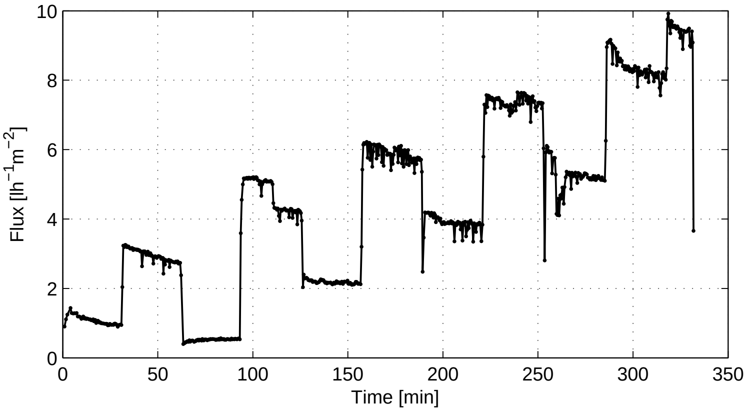

Figure 4.24: Filtration preformed with model particles flocculated with the long polymer (ratio 0.5) and a flow of 0.6 L/min.

Figure 4.24 shows the flux vs. time graph for Long0506. This figure resembles Figure 4.21 very much, thus the same points are valid for this experiment.

Figure 4.25 shows the correlation between flux and pressure for Long0506. Two second degree polynomials are fitted to respectively the average values for the pressure steps: one representant for each of the 1^{st} and one representant for each of 2^{nd} pressure steps. This figure resembles figure 4.23 very much, so the same points is valid for this experiment.

Figure 4.26 shows the pressure profile for Long0506 and the resistance development over time. The resistance development for this experiment looks a lot like the resistance development in Figure 4.23. This indicate that high resistance for the second step at 0.5 bar is not coincidental.

CR 1

Figure 4.27 shows the flux vs. time graph for Long104. The graphs depicts that the step corresponding to 2.5 bar is very messy – it starts low and then becomes very high. Figure 4.29 shows that it is not caused by a mistake in the pressure. However it could be explained by the fact that the flow gauge is not able to keep up with the permeate flow. When this is the case the flux is artificially low, if the

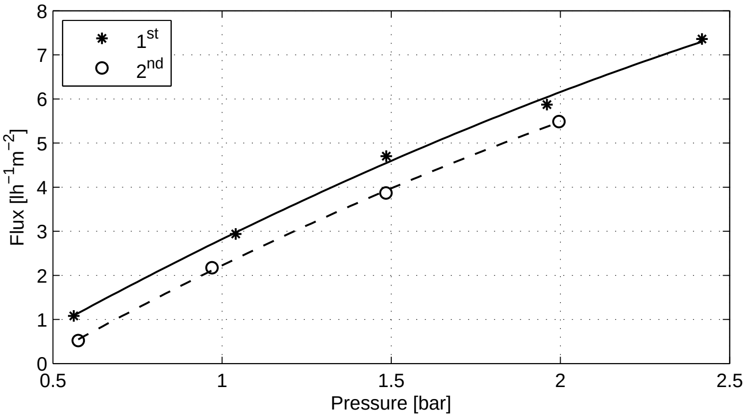

Figure 4.25: Average flux and pressure for each step in the Long0506 experiment. The curves are second degree polynomials fitted to the data points. The notation 1^{st} and 2^{nd} is defined in Figure 3.8. Both polynomials are fitted with R^2 of 0.99.

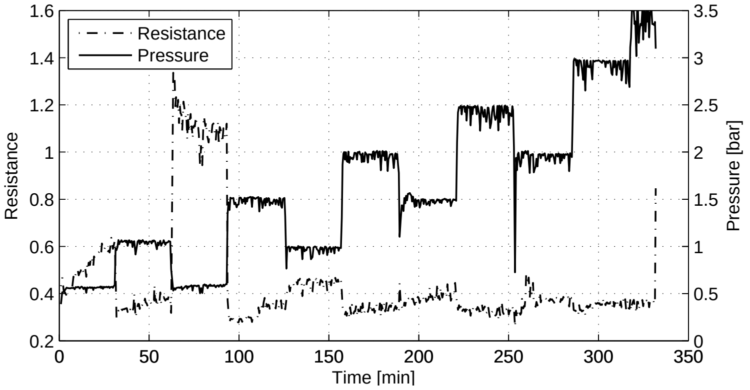

Figure 4.26: Resistance development over time and the pressure over time for the filtration of the long polymer CR 05 and a flow of 0.6 L/min.

flux the decline so the flow is able to keep up an increase in flux will be detected as in Figure 4.27. The generally seems horizontal, thus the critical flux is not reached. This allegation is confirmed by Figure 4.28 which shows the correlation between flux and pressure for Long104. Two second degree polynomials are fitted to respectively the average values for the pressure steps: one representant for each of the 1^{st} and one representant for each of 2^{nd} pressure steps. The two points that are spuriously low are not used when fitting the curves – Thus the few number of points produces very good fits. The curves are nearly identical and they quite linear. This indicates that it is the linear part of the curve and no fouling has

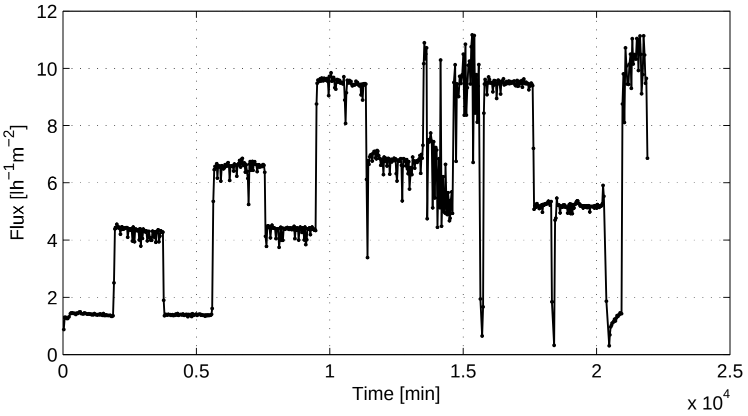

Figure 4.27: Filtration preformed with model particles flocculated with the long polymer (ratio 1) and a flow of 0.4 L/min .

occurred yet.

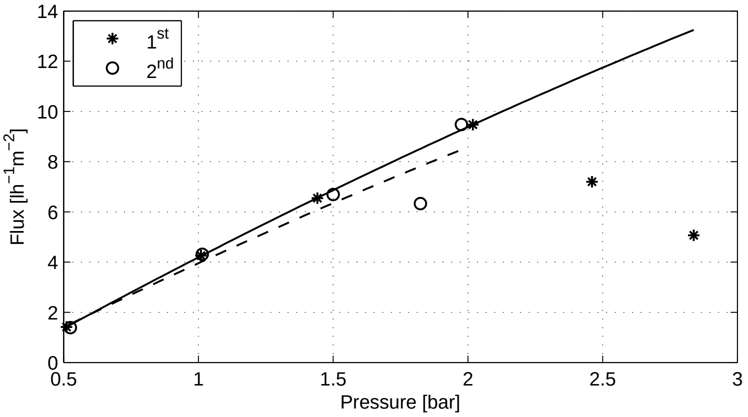

Figure 4.28: Average flux and pressure for each step in the Long104 experiment. The curves are second degree polynomials fitted to the data points. The notation 1^{st} and 2^{nd} is defined in Figure 3.8. The polynomials are fitted with R^2 of respectively 1.00 and 0.90.

Figure 4.29 shows the pressure profile for Long104 and the resistance development over time. Because the resistance is calculated from the flux the resistance becomes artificially high when the flux is artificially low.

Figure 4.30 shows the flux vs. time graph for Long106. The step correspond to 3 bar is messy otherwise the step are horizontal. This means that for the previous experiment that the critical flux can not be found in this study.

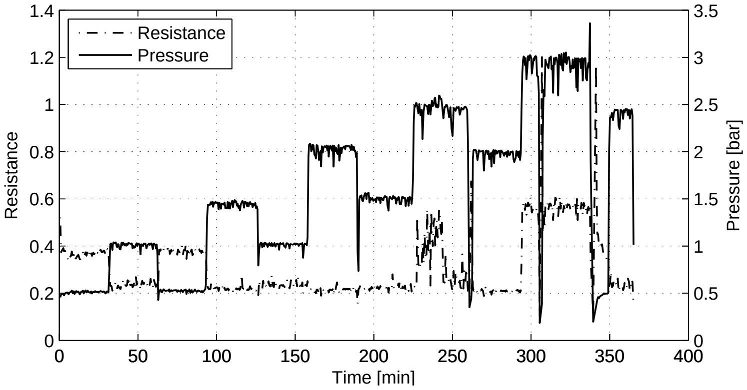

Figure 4.29: Resistance development over time and the pressure over time for the filtration of the long polymer CR 1 and a flow of $0.4\,\mathrm{L/min}$.

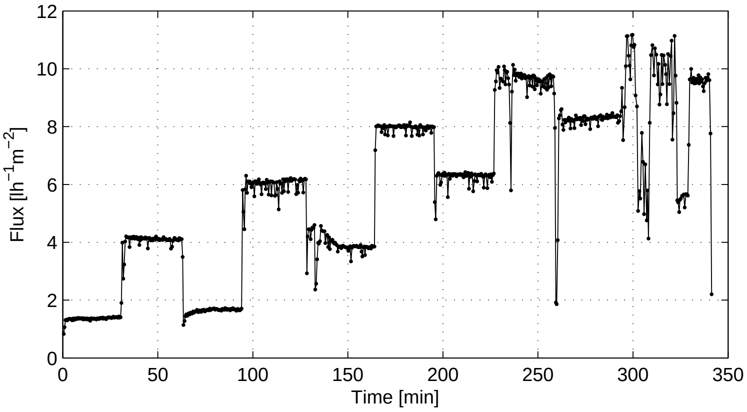

Figure 4.30: Filtration preformed with model particles flocculated with the long polymer(ratio 1) and a flow of $0.6\,\mathrm{L/min}$.

Figure 4.31 shows the correlation between flux and pressure for Long106. Two second degree polynomials are fitted to respectively the average values for the pressure steps: one representant for each of the 1^{st} and one representant for each of 2^{nd} pressure steps. The two curves lie in top of each other indicating no fouling. However, some deposits on the membrane were always observed after an experiment. This could be explained by two different phenomena: 1) There is a very rapid adsorption of the floc to the membrane surface, thus it follows Field *et al.*'s [1995] weaker from of critical flux and afterwards there is no more fouling. 2) The structure of particles cake deposited on the membrane does not influence the resistance. The last of the two possibilities seem highly unlikely, so it is properly the first explanation. Figure 4.31 depicts J_{crit} to be approximately $6\,\mathrm{Lh^{-1}m^{-2}}$.

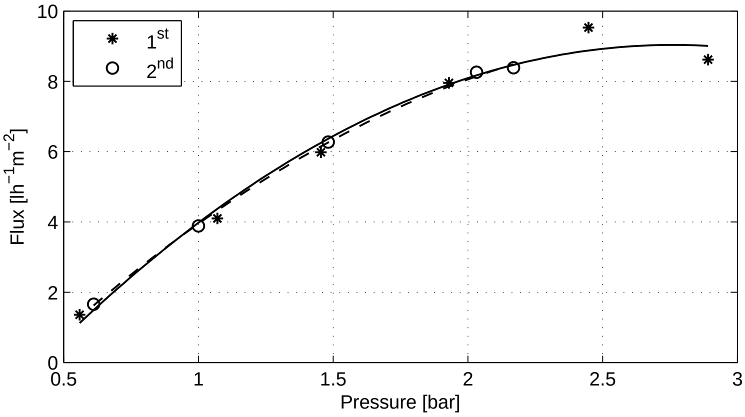

Figure 4.31: Average flux and pressure for each step in the Long106 experiment. The curves are second degree polynomials fitted to the data points. The notation 1^{st} and 2^{nd} is defined in Figure 3.8. The polynomials are fitted with R^2 of respectively 0.98 and 0.99.

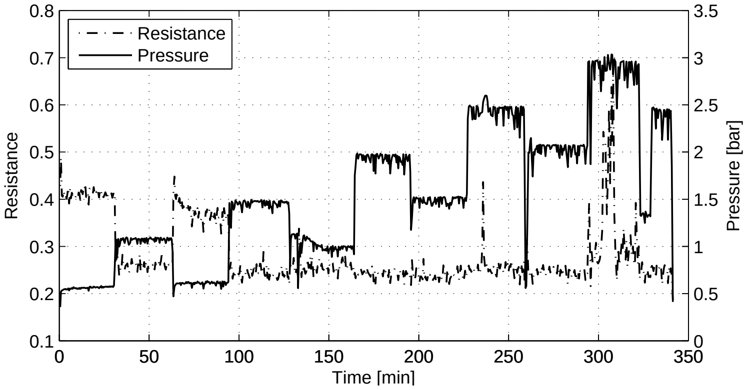

Figure 4.32: Resistance development over time and the pressure over time for the filtration of the long polymer CR 1 and a flow of 0.6 L/min.

Figure 4.32 shows the pressure profile for Long106 and the resistance development over time. When the pressure is 3 bar the resistance makes a peak, which is a result of the messy flow data, see Figure 4.30.

CR 2

Figure 4.33 shows the flux vs. time graph for Long204. All of the steps seem horizontal, thus no indication of fouling. J_{crit} cannot be assessed from this figure. The flux might not have exceeded it. The steps corresponding to 2.5 bar and 3 bar

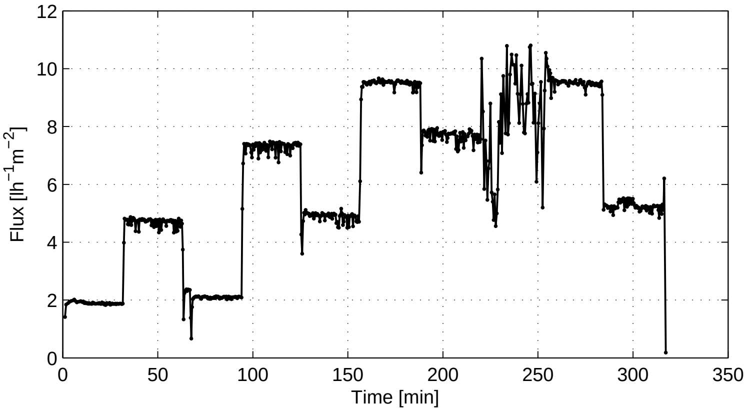

Figure 4.33: Filtration preformed with model particles flocculated with the long polymer(ratio 2) and a flow of $0.4\,\mathrm{L/min}$.

are lower than they should be. This is the result of the flow gauge not being able to keep up with the permeate flow.

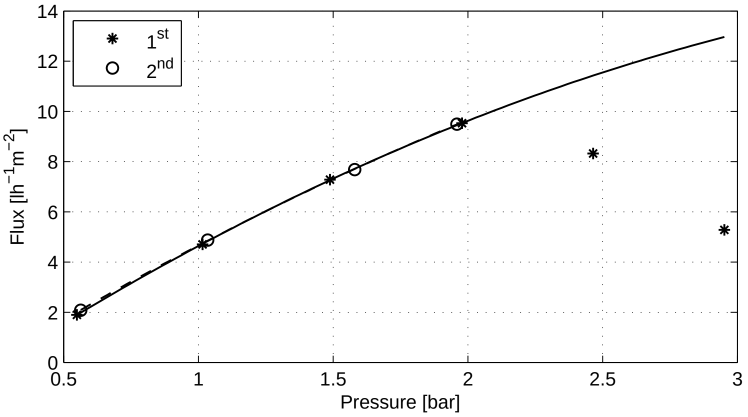

Figure 4.34: Average flux and pressure for each step in the Long204 experiment. The curves are second degree polynomials fitted to the data points. The notation 1^{st} and 2^{nd} is defined in Figure 3.8. The polynomials are fitted with R^2 of respectively 0.95 and 0.99.

Figure 4.34 shows the correlation between flux and pressure for Long204 and a flow velocity of $0.4\,\mathrm{L/min}$. Two second degree polynomials are fitted to the average values for the pressure steps: one represents each of the 1^{st} and one represents each of 2^{nd} pressure steps. The two points which the curve does not go through are not used in the fitting, because as explained in the previous section they are unnatural low. The two curves lie on top of each other, thus no fouling occurs.

However the curve bends off so an approximate assessment of J_{crit} is $8\,\mathrm{Lh^{-1}m^{-2}}$.

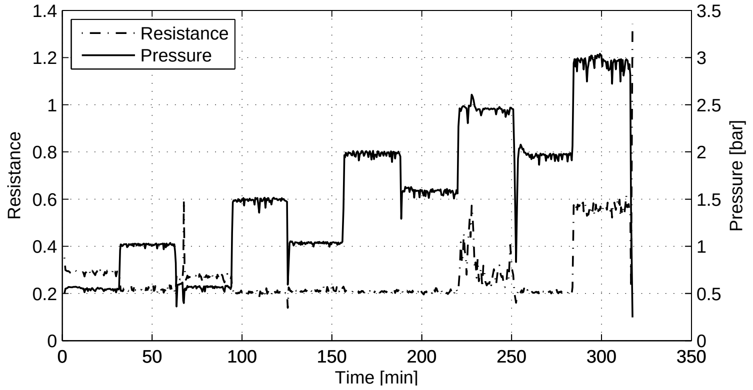

Figure 4.35: Resistance development over time and the pressure over time for the filtration of the long polymer CR 2 and a flow of $0.4\,\mathrm{L/min}$.

Figure 4.35 shows the pressure profile for Long204 and the resistance development over time. The pressure graph looks as expected, however the resistance development have two sudden increases at pressure of 2.5 bar and 3 bar. They are caused by the unnatural low values of the flux for these two steps, see Figure 4.33.

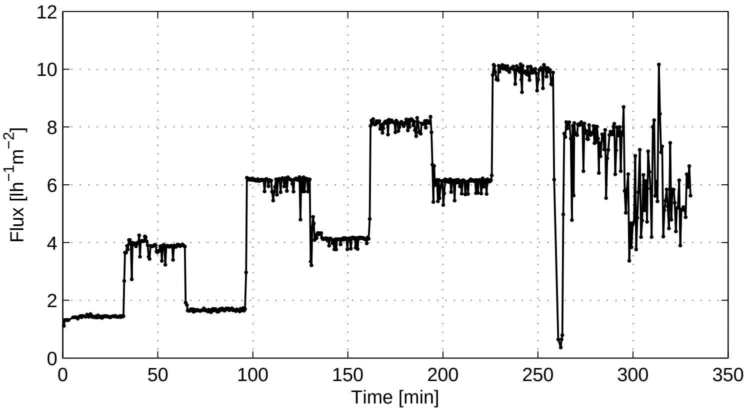

Figure 4.36: Filtration preformed with model particles flocculated with the long polymer(ratio 2) and a flow of $0.6\,\mathrm{L/min}$.

Figure 4.36 shows the flux vs. time graph for Long206. The step corresponding to 3 bar is lower than it should be because the flow gauge cannot keep up with the permeate flow. This is further indicated by the fact that Figure 4.38 shows the pressure is as it should be. All the steps seem horizontal, which mean no fouling occurs. The two lie on top of each other meaning no fouling occurs. However, it does start to bend of, so an approximate assessment of J_{crit} is $7.5\,\mathrm{Lh^{-1}m^{-2}}$.

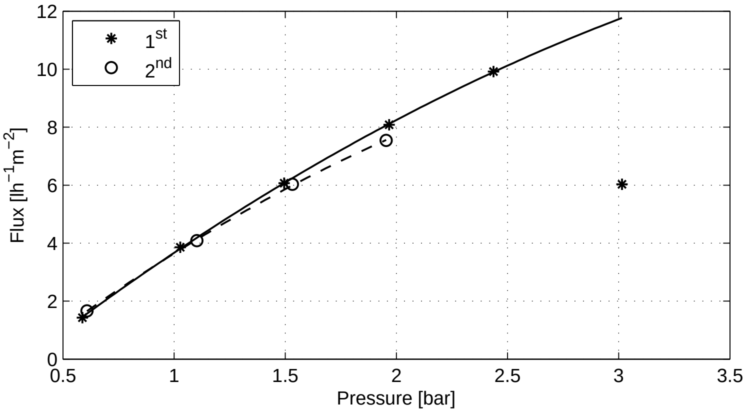

Figure 4.37: Average flux and pressure for each step in the Long206 experiment. The curves are second degree polynomials fitted to the data points. The notation 1^{st} and 2^{nd} is defined in Figure 3.8. The polynomials are fitted with R^2 of respectively 0.90 and 0.99.

Figure 4.37 shows the correlation between flux and pressure for Long206. Two second degree polynomials are fitted to respectively the average values for the pressure steps: one representant for each of the 1^{st} and one representant for each of 2^{nd} pressure steps. The one point that is by itself, is not used during the fitting, because it is unnatural low as explained in the previous section.

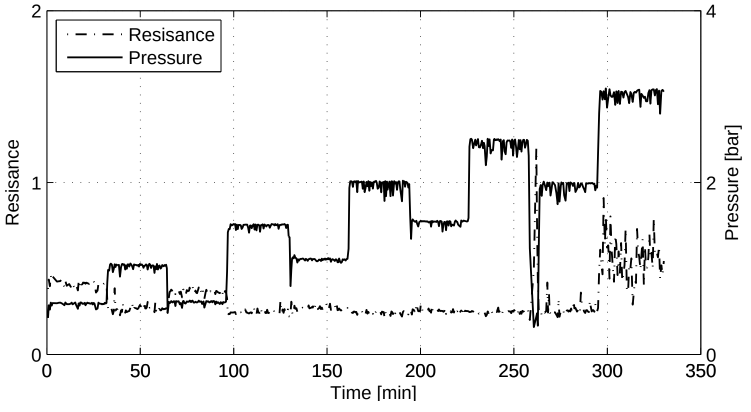

Figure 4.38: Resistance development over time and the pressure over time for the filtration of the long polymer CR 2 and a flow of $0.6\,\mathrm{L/min}$.

Figure 4.38 shows the pressure profile for Long206 and the resistance development over time. The pressure graph looks as expected, however the resistance has a high peak in the end. This is a result of the unnatural low flow for the pressure step at 3 bar.

4.3.4 Cross-linked

The results for the three experiments with the cross-linked polymer as flocculant are displayed in this section. However, the graphs displaying the pressure profiles and the resistance developments over time for these experiments can be found in Appendix B – There is not anything new to comment on them.

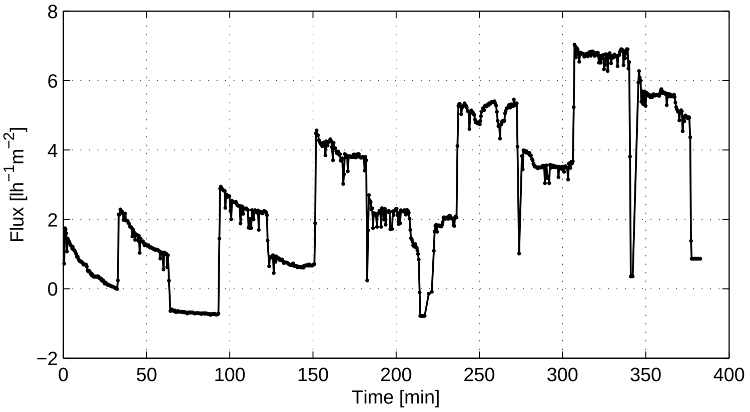

Figure 4.39: Filtration preformed with model particles flocculated with the cross-linked polymer(CR 0.5) and a flow of 0.4 L/min .

Figure 4.39 shows the flux vs. time graphs for Cross0504. The figure depicts that the flux drop to near zero at the first step, which must be because of some reversible blockage of the membrane. This causes a massive increase in the resistance at first as Figure B.1 shows followed by a drop in the resistance as the pressure is increased. Hence the blockage was reversible. Though it is not the expected behavior, normally the drop would be expected after a pressure drop because then the particles are easier to remove from the membrane.

The duration time for the second step equivalent to a pressure of 1.5 bar is longer that the usually 30 min because of a failure of the pump outside the main system. This resulted in loosing fluid from the system. The fluid was returned into the system by adding an extra pump. All the steps in this experiment seem to have a slope meaning that the J_{crit} is below the sensitivity of the pressure gauge.

Figure 4.40 shows the flux vs. time for Cross104. The flux is high compared with the experiments described previously in this chapter, but the steps are tilted so the critical flux exists below the detectable limited for these experiments. After the

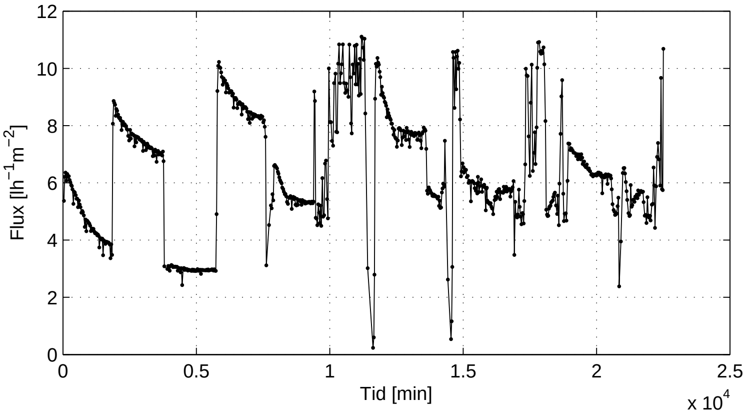

Figure 4.40: Filtration preformed with model particles flocculated with the cross-linked polymer(ratio 1) and a flow of $0.4\,\mathrm{L/min}$.

second step at 1 bar the data becomes messy. This may be caused by a wet circuit board.

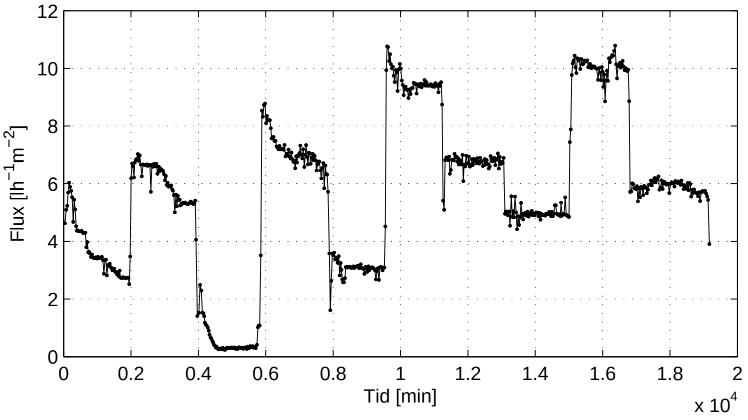

Figure 4.41: Filtration preformed with model particles flocculated with the cross-linked polymer (ratio 2) and a flow of $0.4\,\mathrm{L/min}$.

Figure 4.41 shows the flux vs. time for Cross204. For this experiment the flocs seem to be adsorbed to the inner surface of the flow gauge. The flow gauge is made from see-trough plastic and during the experiment it became white. It was difficult to remove the flocs after the experiment was done. The system was cleaned with a solution with high NaCL contents in addition to the conventional method (see Section 3.5.3). As it also applies to the other two experiments using the cross-linked polymer, the flux is high compared with the experiments using the long polymer as flocculant. However, it has no horizontal steps, thus critical flux exists below the detectable limited for these experiments. The step corresponding to the pressure 3 bar is lower than expected. This is because the flow gauge cannot keep up with the flow of permeate, causing it to show a lower value than what it really is.

4.3.5 Short Polymer

This section presents the data from the experiments using the short polymer as a flocculant. However, as mentioned in the previous section the time series of pressure and resistance are rather monotonous, and therefore they can be found in Appendix B.

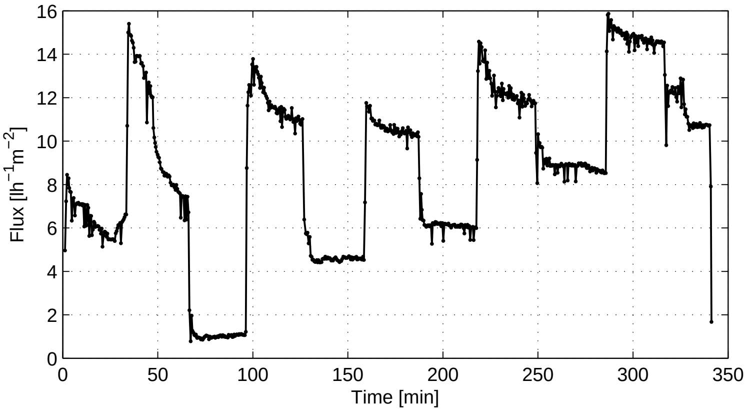

Figure 4.42: Filtration preformed with model particles flocculated with the short polymer (ratio 0.5) and a flow of 0.4 L/min .

Figure 4.42 shows the time series of flux for Short0504. The steps corresponding to the pressures 2.5 bar and 3 bar are artificially low because the pressure gauge cannot keep up with the permeate flow. All of the first steps seem to have a slope meaning J_{crit} is under the detectable limited for the experiment.

Figure 4.43 shows the flux vs. time for Short104. The steps above 1.5 bar are artificially low because the flow could not keep up, and the permeate flow exceeds the maximum capacity for the flow gauge. The starting flux for this experiment is very high, but it decreases rapidly. This means that J_{crit} is below delectability for this experiment.

In the experiment Short204, the experimental setup was modified from the other experiments. In the two previous experiments the permeate flow was too high for the flow gauge to keep up. To avoid that with this experiment, the membrane area was reduced by a factor 2. Practically, this means that two layers of thin plastic (from a small clear plastic bag) was used to block the second membrane area in

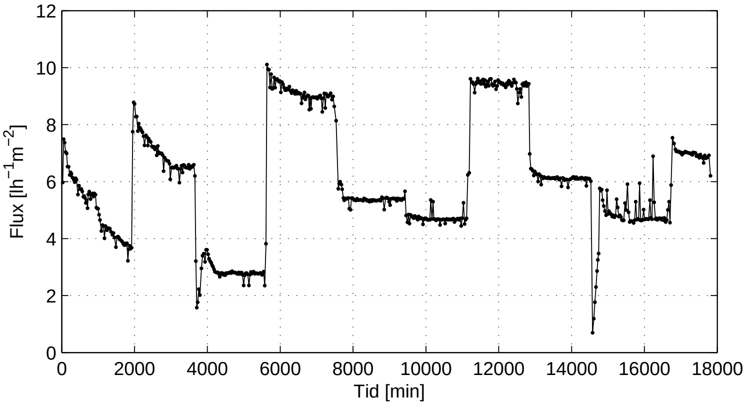

Figure 4.43: Filtration preformed with model particles flocculated with the short polymer (ratio 1) and a flow of 0.4 L/min .

the membrane housing. To ensure comparability with the other two experiments, the half membrane area was used when calibrating the data.

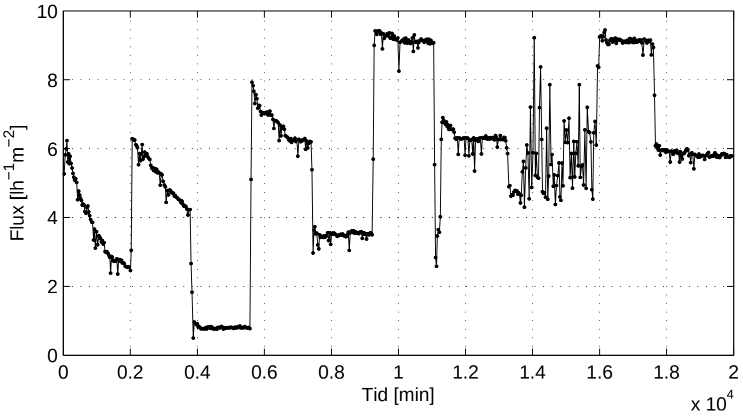

Figure 4.44: Filtration preformed with model particles flocculated with the short polymer (ratio 2) and a flow of 0.4 L/min .

Figure 4.44 shows the time series of flux for the Short204 experiment. In the first step corresponding to the pressure 2.5 bar the data become messy. The flux level for this step and the step corresponding to 3 bar show that the flow gauge has trouble keeping up with the permeate flow despite of the precautions made. The steps corresponding to the first pressures $0.5-1.5$ bar have steep slopes, indicating that J_{crit} is at a pressure below 0.5 bar. The step does not reach J_{ss}, however when the pressure is lowered the step is horizontal. The steps above 1.5 bar are horizontal as well, indicating that the maximum degree of fouling is reached.

Chapter 5

Discussion

The discussion in this chapter is divided into four topics each discussed in a separate section. The data was presented in the previous chapter, but in each of the following sections the data is presented in an alternative form, which illustrates the discussed topics and makes direct comparisons.

5.1 Critical Flux

The critical flux is defined in Section 2.1.4. For all the experiments, the approximate J_{crit} is assessed, and a comparison is shown in Table 5.1.

	CR 0.5	**CR 1**	**CR 2**
Long polymer 0.4 L/min	$J_{crit} < 1.7$	*	8
Long polymer 0.6 L/min	$J_{crit} < 1.7$	6	7.5
Cross-linked polymer	$J_{crit} < 1.8$	$J_{crit} < 6.1$	$J_{crit} < 6$
Short polymer	$J_{crit} < 6.1$	$J_{crit} < 5.9$	$J_{crit} < 6$

Table 5.1: J_{crit} $[\mathrm{Lh^{-1}m^{-2}}]$ for each of the experiments. The asterisk (*) indicates an undeterminable critical flux.

It is possible to assign a value to J_{crit} only for three of the experiments. For the rest of the experiments it is only possible to assess an upper limit for J_{crit}. It is not possible to give a more precise evaluation. The experiment using the long polymer and flow velocity $0.6\,\mathrm{L/min}$ indicates that J_{crit} increases with the increasing polymer dosages. The same can be said for the experiment using the long polymer and flow velocity $0.4\,\mathrm{L/min}$. The rest of the experiments do not indicate anything about the influence of the concentration ratio.

From a comparison between the six different experiments using the long polymer, it seems as if the crossflow velocity does not influence J_{crit} significantly. The effect of the crossflow velocity is expected to be larger than indicated by the data.

5.2 Effect of Concentration Ratio

To evaluate the effect of the concentration ratios on the filtration, four different graphs are displayed on Figures 5.1-5.4. The figures show flux versus pressure for the three CR of each of the polymers and for water. The curves in the plots are quadratic fits to the data set for each of the experiments. However, for water a linear regression is used.

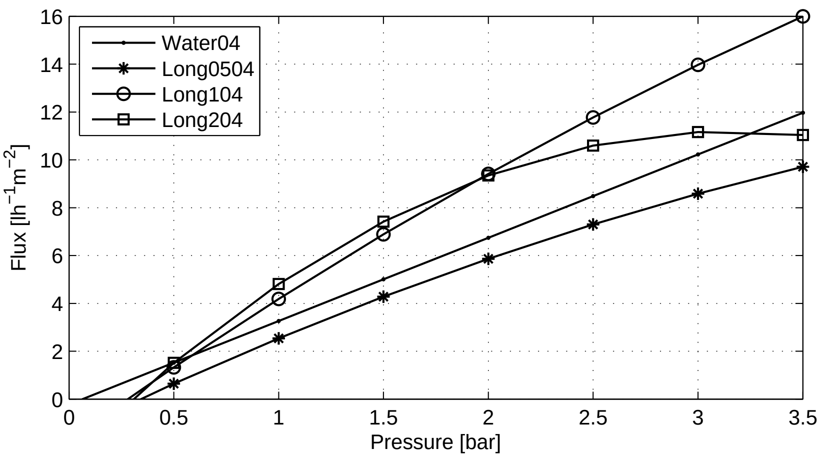

Figure 5.1: Linear fit for water and polynomial fits for the three different concentration ratios. The long polymer is used and the crossflow is 0.4 L/min.

Figure 5.1 shows the curves fitted for three experiments made using the long polymer and a crossflow velocity of 0.4 L/min. The CR 0.5 is the only one below the water line. This is surprising because they all should be equal to or below the water line. It can be caused by the membrane not being uniform so the membrane samples might not be identical from experiment to experiment. Further, it is seen that the curve for CR 0.5 is the lowest one of the three concentration ratios and the other two are quite similar.

Figure 5.2 shows the polynomials fitted to the data from the experiments performed with the long polymer as flocculant and a flow velocity of 0.6 L/min. Again, the three curves for the flocculated experiments are expected to lie below the water line. The CR 0.5 is where it is expected to be, but the other two are higher than the water line. When comparing Figure 5.2 to Figure 5.1 it is seen that they are

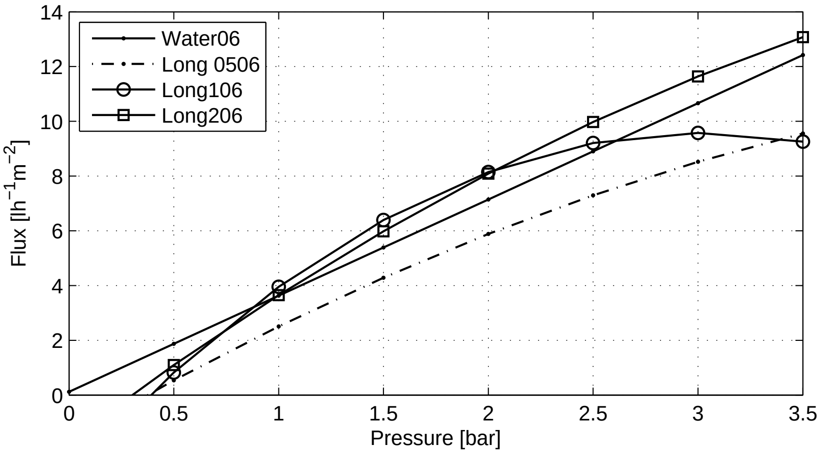

Figure 5.2: Linear fit for water and the non-filtrated particles along with polynomial fits for the three different concentration ratios of the long polymer. The flow is 0.6 L/min.

actually quite similar. In both figures are the curves for CR 0.5 below the water line and the two other curves are quite similar and lie above the water line.

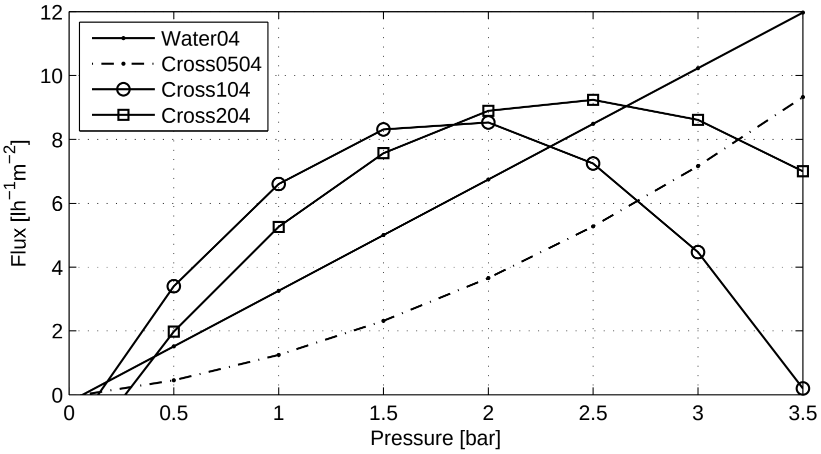

Figure 5.3: Linear fit for water and polynomial fits for the three different concentrations ratios of the cross-linked polymer. The crossflow velocity is 0.4 L/min. The curves for Cross104 and Cross204 are only valid up to a pressure of 2 bar.

Figure 5.3 shows the three fitted curves for the experiments preformed with the cross-linked polymer as flocculant and the water line. The curves for Cross104 and Cross204 are only valid up to a pressure of 2 bar. These two curves are not fitted to all data points from the experiments; because of failure of the flow gauge the last points are not valid, so the last part of the curves are extrapolated. None of the three curves follow the expected pattern. Both curves for CR 1 and 2 exceed the the water line and CR 0.5 is concave.

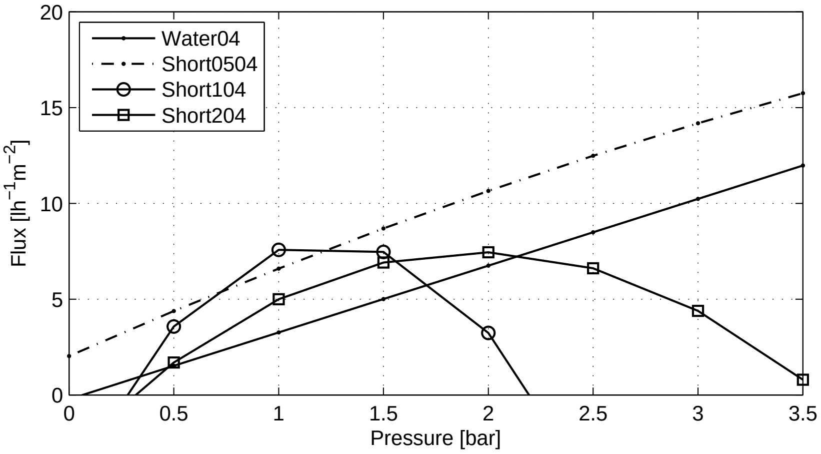

Figure 5.4: Linear fit for water and the polynomial fits for the three different concentration ratios for the short polymer. The crossflow velocity is 0.4 L/min. The curves for Short104 and Short204 are only valid for pressures up to 1.5 bar and 2 bar, respectively.

Figure 5.4 shows the water line and the polynomials fitted to the data for the experiments with the short polymer. As for Figure 5.3 some data points were left out when fitting the polynomials because of failure of the flow gauge. This explains why the curves for CR 1 and 2 are highly concave and do not follow the theory in Section 2.1. They should only be trusted up to a pressure of $1.5-2$ bar.

The curve for CR 0.5 lies above the line for water and this is different from the other three figures in this section. The fit is extrapolated from a small amount of data points, because as it can be seen from Figure 4.42 the data is very unstable. This can be caused by a wet circuit board, but it does not explain why the CR 0.5 is that much higher than the water line.

Summary and Comparison

Ignoring the figures shown in this section for a moment and instead looking a the plots of flux vs. time from Section 4.3 makes the tendency is much clearer. The reason for this is not known.

For the long polymer at both flow rates it applies that the un-flocculated particles have the lowest fluxes at the respective pressures, and that the CR 0.5 definitely increases the suspensions ability to be filtrated. In both cases are CR 1 very similar to the the water line. There are small differences between the CR 1 and 2, and the

CR 2 seems to have slightly better filtration ability. Sometimes it even exceeds the water lines. From a comparison with the theory described in Section 2.1 it could be estimated that the part which exceeds water is in fact the same as water. The difference between them could be in the non-uniformity of the membrane and the sensitivity of the laboratory system. For both the cross-linked polymer and short polymer experiments it is hard to detect any clear tendencies.

5.3 Concentration Ratio vs. Flow Velocity

To investigate how the crossflow velocity influences the filtration, five experiments were carried out at two different crossflow velocities. The experiments are the ones with demineralized water, the ones with un-flocculated particles and the three with the long polymer as flocculant (CR 0.5, CR 1 and CR 2). The experiments with water are displayed in Figure 4.14 are quite similar which is expected from the theory, cf. 2.1, because the only resistance is from the membrane and it does not change with the crossflow. All the data from experiments where a flocculant is used is expected to lie between the curve for the demineralized water and the un-flocculated particles. The curves for the un-flocculated particles are not shown in this Section and compared to the others, because the data from these experiments has not been calibrated. It can be seen in Figures 4.16 and 4.19. If comparing all the data before calibration (the data relative to each other) the un-flocculated have the lowest fluxes, and there is a difference between the two of them. The one with the lowest crossflow velocity has the lowest flux. This is the expected result because of the lower drag force away from the membrane caused by the lower crossflow, and thus a larger quantity of particles can settle onto the membrane.

Figure 5.5 shows all the experimental data from the experiments using the long polymer as flocculant. The curves are fitted to the average flux for each pressure. The curves for the experiments with CR 0.5 lie on top of each other, and represents the lowest curve. The rest of the curves follow each other unto the bend off. The Long104 bends off before Long106, and the remaining two do not bend off in this graph. Hence, the crossflow does not effect Long0504 and Long0506, however it does seem to influence the other experiments.

5.4 Effect of Polymer Structure

One of the main purposes of this thesis is to investigate how the polymer structure influences the ability of the suspension to be filtrated – Another is to investigate the influence of the molecular weight. To investigate these two purposes three different polymers are used for the experiments. From Section 2.1 it can be seen that there are three different structures of polymers, but this thesis only investigates the two of them. The linear which Section 2.1 states is the most common used and a cross-

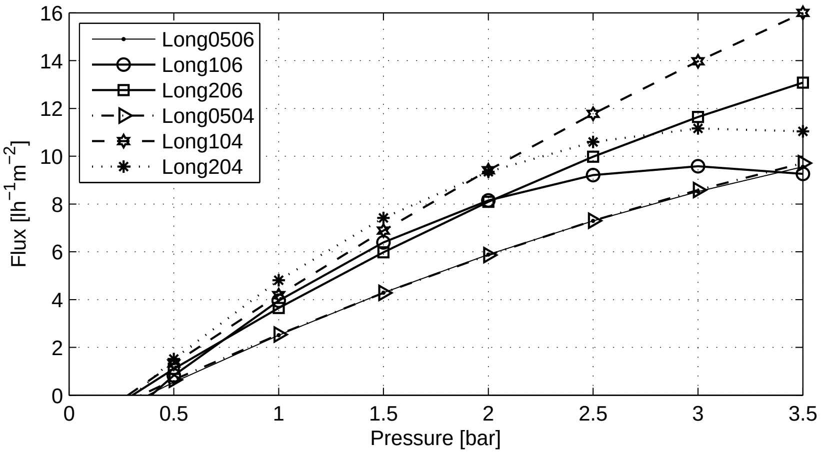

Figure 5.5: Polynomial fits for the three different concentration ratios for the long polymer at both the flow velocities.

linked. To investigated the molecular weight short and long chained polymers are selected. Even though they do not have the same monomeric unit they will be compared. In this Section three different graphs are displayed. They each show three different curves; one for each type of polymer used for the experiments made with a crossflow velocity of $0.4\,\mathrm{L/min}$.

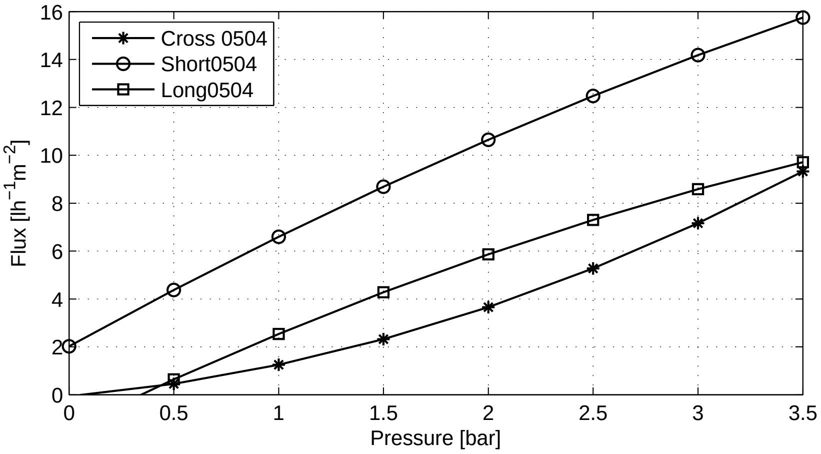

Figure 5.6: Polynomial fits for the three different polymers with a concentration ratio of 0.5 and a flow of $0.4\,\mathrm{L/min}$.

Figure 5.6 shows the curves for CR 0.5. The line for Short0504 lies well above the other two while Long0504 is higher than Cross0504.

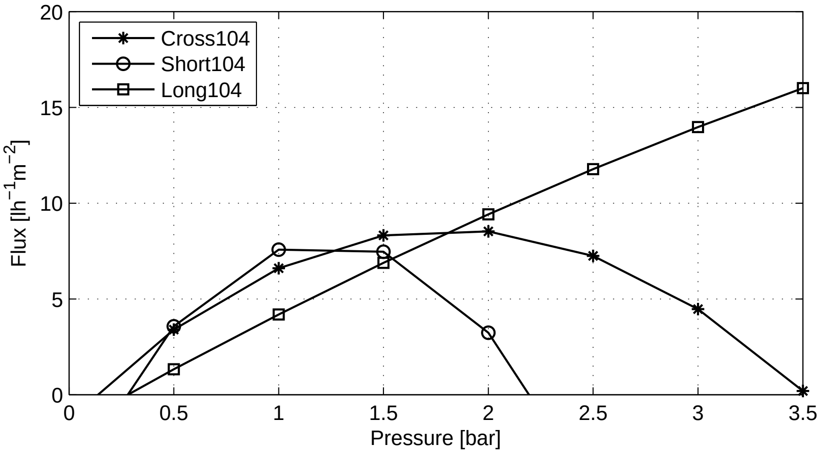

Figure 5.7: Polynomial fits for the three different polymers with a concentration ratio of 1 and a flow of 0.4 L/min. The curves for Short104 and Cross104 are only valid up to pressures of 1.5 bar and 2.0 bar, respectively.

Figure 5.7 shows the curves for CR 1. They look alike in the beginning and the Cross104 and Short104 bend off approximately at the same time. Long104 does not bend off at all.

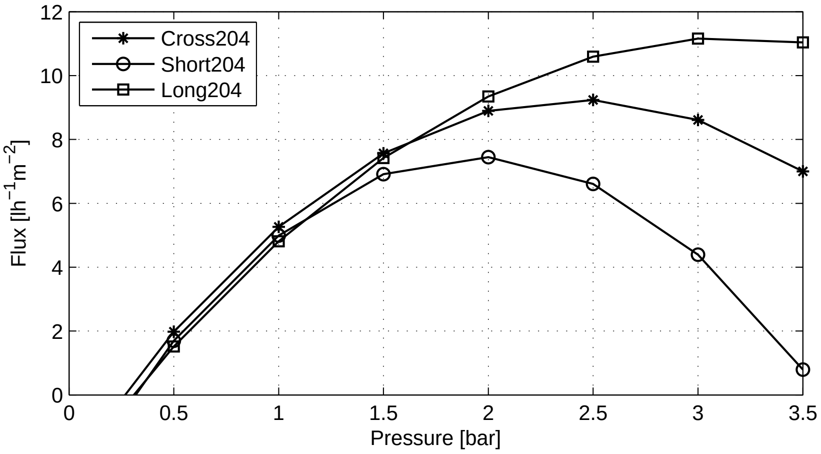

Figure 5.8: Polynomial fits for the three different polymers with a concentration ratio of 2 and a flow of 0.4 L/min. The curves for Short204 and Cross204 are only valid up to pressures of 2.0 bar.

Figure 5.8 shows the curves for CR 2. All three of them follow each other in the beginning. Short204 bend off before Cross204, and Long204 does not bend off in this graph.

Summary and Comparison

The polymeric structure does influence ability of the suspension to be filtrated. Both Figure 5.7 and Figure 5.8 show that the long polymer gives the best results and this matches well with [Gregory 2006] which states that often long straight polymers are used for flocculation. It is hard to se any other indications with respect to the polymer structure.

The ability of the suspension to be filtrated seems to increase as the molecular weight increases, but the data does not allow it to be discussed more thoroughly.

Chapter 6

Conclusion

Based on the experimental results gathered in this thesis, multiple conclusions can be drawn.

The use of a flocculant increases the ability of a polystyrene particles suspension (particle size range $400-500\,\text{nm}$) to be filtrated. When the particles are flocculated the size range increases to $7-700\,\mu\text{m}$. The more precise range depends upon the type of polymer and concentration.

Two different flocculant structures were evaluated; a straight (Zetag 7631, Ciba) and a cross-linked (Zetag 7867FS40, Ciba (Poly(acryloxyethyltrimethyl ammonium chloride-co- acrylamide))). This thesis finds that the straight one is the best of the two.

Evaluation of the influence of molecular weight on the filtration was done by comparing two different straight polymers; a long chained polymer (Zetag 7631, Ciba) and a short chained polymer (polyDADMAC). The results were inconclusive.

Evaluation of the influence of the crossflow on the filtration was done by preforming otherwise identical experiments and varying the flow velocity. Two different velocities were investigated, namely $0.4\,\text{L}/\text{min}$ and $0.6\,\text{L}/\text{min}$. It seems to have a little effect.

The polymer dosage was also investigated. The dosage was based on charge ratio (CR), to be able to compare the results across the polymer types. Three different CR were investigated; CR 0.5, CR 1, and CR 2. The criteria used to assess the charge ratios is the critical flux (J_{crit}). J_{crit} seems to increase with an increase of the CR.

Bibliography

Aimar, P. & Bacchin, P. [2010], ‘Slow colloidal aggregation and membrane fouling’, *Journal of Membrane Science* **360**, 70–76.

Andersen, M. B. O. & Nielsen, T. B. [2007], Cross-flow microfiltration of poly(styrene-co-acrylic acid) with varying acrylic acid shell thickness, Technical report, Aalborg University.

Atkins, P. & De Paula, J. [2006], *Atkins’ Physical Chemistry*, 8th edn, Oxford Pniveristy Press.

Bacchin, P., Aimar, P. & Field, R. [2006], ‘Critical and sustainable fluxes: Theory, experiments and applications’, *Journal of Membrane Science* **281**, 42–69.

Bacchin, P., Aimar, P. & Sanchez, V. [1995], ‘Model for colloidal fouling of membranes’, *AIChE Journal* **41**, 368–377.

Chellappah, K., Tarleton, E. & Wakeman, R. [2008], ‘Effect of flocculation on critical flux during crossflow microfiltration of bentonite suspensions’, *Separation Science and Technology* **43**, 29–44.

Cheryan, M. [1998], *Ultrafiltration and Microfiltration: Handbook*, Technomic Publishing Company, Inc.

Christensen, P. V., Hinge, M. & Keiding, K. [2009], ‘The use of dielectric spectroscopy in the investigation of the effect of polymer choice on the flocculation of polystyrene particles’, *Journal of Colloid and Interface Science* **331**, 113–121.

Christensen, P. V. & Keiding, K. [2008], ‘The use of dielectric spectroscopy for the characterization of polymer-induced flocculation of polystyrene particles’, *Journal of Colloid and Interface Science* **327**, 362–369.

Christensena, M. L., Hjorth, M. & Keiding, K. [2009], ‘Characterization of pig slurry with reference to flocculation and separation’, *Water Research* **43**, 773Ű783.

Clement, K. H., Fangel, P., Jensen, A. D. & Thomsen, K. [2004], *Kemiske enhedsoperationer*, Polyteknisk forlag.

Espinasse, B., Bacchin, P. & Aimar, P. [2002], ‘On an experimental method to measure critical flux in ultrafiltration’, *Desalination* **146**(9), l–96.

Field, R., WU, D., Howell, J. & Gupt, B. [1995], ‘Critical flux concept for microfiltration fouling’, *Journal of Membrane Science* **100**, 259–272.

Gregory, J. [2006], *Particles in water porperties and processes*, CRC Press.

Holm, J. [2009], Microfiltration of poly(styrene) and poly(styrene-co-acrylic acid) core-shell particles in cross-flow system: A contribution to prediction of the fouling resistance, with a varying ψ_f content, Master’s thesis, Aalborg University.

Howell, J. A. [1995], ‘Sub-critical flux operation of microfiltration’, *Journal of Membrane Science* **107**, 165–171.

Jarvis, P., Jefferson, B., Gregory, J. & Parsons, S. [2005], ‘A review of floc strength and breakage’, *Water Research* **39**, 3121Ű3137.

Kam, S.-k. & Gregory, J. [1999], ‘Charge determination of synthetic cationic polyelectrolytes by colloid titration’, *Colloids and Surfaces A: Physicochemical and Engineering Aspects* **159**, 165Ű179.

Laval, A. [2006], Cleaning of dss flat sheet membranes, Technical report, Alfa Laval.

Appendices

Appendix A

MATLAB Code

This chapter contains an explanation of the MATLAB code used for analyzing the data. All of the data sets are analyzed identically. Furthermore, an explanation for discarding data points and displaying the data as chosen is given here.

Below, the commands of the script are shown and a description is given. The script for the experiment with water at the flow velocity $0.4\,\mathrm{L/min}$ is used as en example.

First, the raw data is read from the txt file and is a matrix where column 1 is the time in sec, column 2 is the pressure in bar and column 3 is the flow though the membrane in $\mathrm{L/min}$:

```
filename='C:\...\Master\data\vand04data.txt';
data=dlmread(filename,'\ ',10,0);
```

Data column 3 is read and calibrated by the function found in Section 3.5.2 and the flow ($\mathrm{L/min}$) is changed to flux with the unit ($\mathrm{L/hm^2}$) by division of the membrane area:

```
data(:,3)=(data(:,3)*0.0202-0.0527)/0.0188;
```

Next, both the pressure and the flux time series are modified in the same way. Therefore it is done in a loop, so the same code is used for both channels. There are three steps:

1. Plot the raw data.
2. Discard negative data points and outliers defined by the variable `eps`.
3. Compute running average.

In each of the three steps the data is plotted and the resulting plots are shown in Figure A.1. Lines starting with a `%` are comments.

```
m=20; % Number of points in running average
for nr=2:3
    % -------------------------------------------------------------
    % Define filenames, label for the 2nd axis and a threshold for
    % discarding data points. These variables are different for
    % pressure and flux - Therefore are they defined inside the
    % for-loop.
    % -------------------------------------------------------------
    if nr==2
        figurnavn='tryk';
        ytext='Pressure [bar]';
        eps=0.2; % cutoff for outliers
    else
        figurnavn='';
        ytext='Flux [lh^-^1m^-^2]';
        eps=2;% cutoff for outliers
    end
    % -------------------------------------------------------------
    % STEP 1: Make plot of the raw data
    % -------------------------------------------------------------
    figure
    plot(data(:,1),data(:,nr),'k.')
    xlabel('Time [sec]')
    ylabel(ytext)
    grid on
    % -------------------------------------------------------------
    % STEP 2: Removal of negative data points and outliers
    % -------------------------------------------------------------
    % STEP 2.1 removal of negative outliers
    N=size(data,1);
    for i=N:-1:2
        if or(data(i,nr)<data(i-1,nr)-eps,data(i,nr)<0)
            data(i,:)=[];
        end
    end
    % STEP 2.2 removal of positive outliers
    J=size(data,1);
    for i=J:-1:2
        if data(i,nr)> eps+data(i-1,nr)
            data(i,:)=[];
        end
    end
    % FIGURE 2 - Plot the data
    figure
    plot(data(:,1)/60,data(:,nr),'k.-')
    xlabel('Time [min]')
    ylabel(ytext)
```

```
    grid on
    % ----------------------------------------------------------------
    % STEP 3: Compute running average over 'm' data points
    % ----------------------------------------------------------------
    K=size(data,1);
    L=floor(K/m);
    newdata=zeros(L,size(data,2));
    for i=1:L
        newdata(i,:)=mean(data(1+(i-1)*m:i*m,:),1);
    end
    % FIGURE 3 - Plot the data
    plot(newdata(:,1)/60,newdata(:,nr),'k.-')
    xlabel('Tid [min]')
    ylabel(ytext)
    grid on
end
```

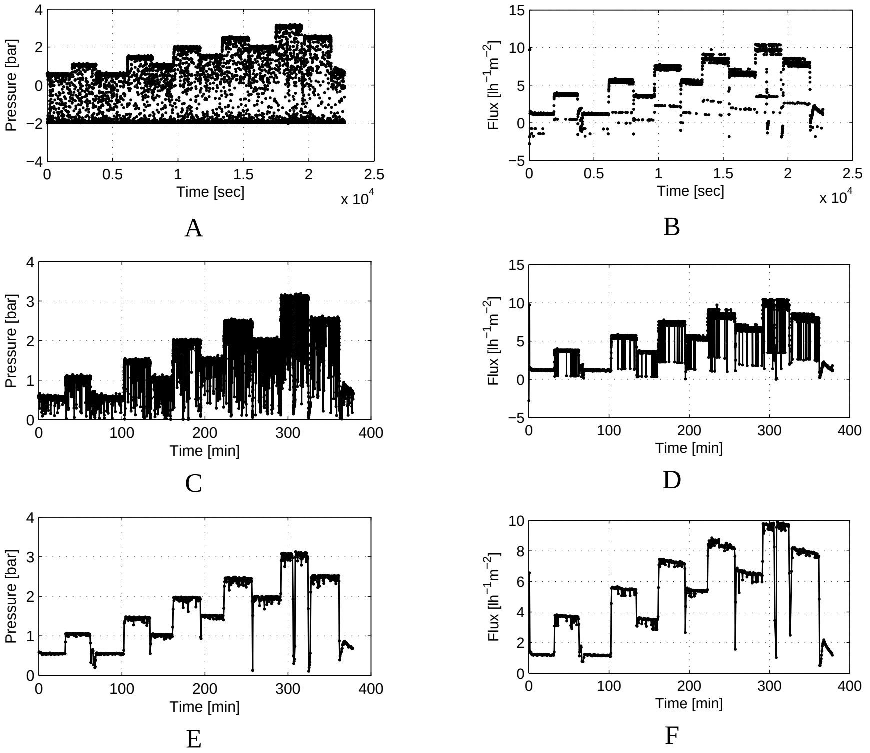

Figure A.1: A: Raw data from pressure transducer. B: Raw data from flow gauge after calibration. C & D: Negative data points and outliers have been discarded. E & F: Running mean over 20 data points.

From each step of the experiment, the mean pressure and mean flux is computed. The start and end indices for each step is read manually from the underlying data set. The mean flux in each step is plotted against the corresponding pressure as shown in Figure A.2.

```
% ----------------------------------------------------------------
% Determine mean values for first step at given pressure
% ----------------------------------------------------------------
% Pressure
avg05p=mean(newdata(1:65,2));
avg1p=mean(newdata(67:130,2));
avg15p=mean(newdata(219:282,2));
avg2p=mean(newdata(345:409,2));
avg25p=mean(newdata(471:540,2));
avg3p=mean(newdata([616:654 654:676],2));
avgp1=[avg05p avg1p avg15p avg2p avg25p avg3p];
% Flow
avg05f=mean(newdata(1:65,3));
avg1f=mean(newdata(67:130,3));
avg15f=mean(newdata(219:282,3));
avg2f=mean(newdata(345:409,3));
avg25f=mean(newdata(471:540,3));
avg3f=mean(newdata([616:654 654:676],3));
avgf1=[avg05f avg1f avg15f avg2f avg25f avg3f];
% ---------------------------------------------------------------
% Determine mean values for second step at given pressure
% ---------------------------------------------------------------
% Pressure
avg05p2=mean(newdata(133:213,2));
avg1p2=mean(newdata(205:338,2));
avg15p2=mean(newdata(412:469,2));
avg2p2=mean(newdata(544:614,2));
avg25p2=mean(newdata(682:752,2));
avgp2=[avg05p2 avg1p2 avg15p2 avg2p2 avg25p2];
% Flow
avg05f2=mean(newdata(133:213,3));
avg1f2=mean(newdata(205:338,3));
avg15f2=mean(newdata(412:469,3));
avg2f2=mean(newdata(544:614,3));
avg25f2=mean(newdata(682:752,3));
avgf2=[avg05f2 avg1f2 avg15f2 avg2f2 avg25f2];
% ---------------------------------------------------------------
% Fit curves through the points
% ---------------------------------------------------------------
[P1,R1]=polyfitRsq(avgp1,avgf1,1);
[P2,R2]=polyfitRsq(avgp2,avgf2,1);
% ---------------------------------------------------------------
```

```
% Make plot
% ---------------------------------------------------------------
fh=figure;
plot(avgp1,avgf1,’k*’,’linewidth’,1)
hold on
plot(avgp2,avgf2,’ko’,’linewidth’,1)
hold on
x1=linspace(min(avgp1),max(avgp1));
plot(x1,P1(1)*x1+P1(2),’k-’,’linewidth’,1)
hold on
x2=linspace(min(avgp2),max(avgp2));
plot(x2,P2(1)*x2+P2(2),’k--’,’linewidth’,1)
xlabel(’Pressure [bar]’)
ylabel(’Flux [lh^-^1m^-^2]’)
grid on
legend(’1^{st}’,’2^{nd}’,’Location’,’NorthWest’)
```

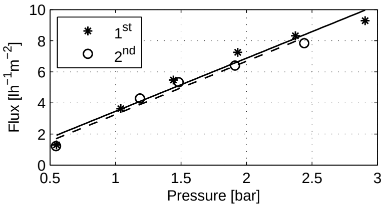

Figure A.2: Mean values from each step.

A new vector is computed by dividing the pressure with the flux. This vector shows the resistance development over time. The resistance and the pressure are plotted in the same figure, Figure A.3.

```
modstand=newdata(:,2)./newdata(:,3);
fh=figure;
[ax,h1,h2]=plotyy(newdata(:,1)/60,modstand,newdata(:,1)/60,
newdata(:,2));
set(ax,’YColor’,[0 0 0])
set(get(ax(1),’Ylabel’),’String’,’Resistance’)
set(get(ax(2),’Ylabel’),’String’,’Pressure [bar]’)
set(get(ax(1),’Xlabel’),’String’,’Time [min]’)
grid on
set(h1,’Color’,[0 0 0],’LineStyle’,’-.’,’LineWidth’,lw)
set(h2,’Color’,[0 0 0],’LineStyle’,’-’,’LineWidth’,lw)
legend(’Resistance’,’Pressure’,’Location’,’NorthWest’)
grid on
```

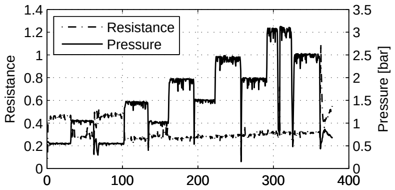

Figure A.3: The resistance development over time for the filtration preformed with water and a flow of $0.4 \mathrm{L/min}$.

Appendix B

Pressure Graphs

The pressure have been monitored in everyone of the experiments. They should all have been identical to figure 3.8 but there are some small differences. These are present because it is difficult to adjust the air pressure correct and every time the pressure have to be lowered all the air must first be let out of the system and then the pressure can be adjusted. Also there are some difficulties when collection the data, it seems as if there are some interferences with the data signal because if often shows the the pressure is -2 and this is the value it shows when there are no signal at all. How the data is treated to give a readable outcome can be seen in appendix A. All the graphs in this appendix also contains the resistance development over time for that experiment.

B.1 Cross-linked

Figure B.1 shows the pressure and resistance development over time for the experiment using the cross-linked flocculant (CR 0.5) and the crossflow velocity of $0.4\,\mathrm{L/min}$. Figure B.1 shows the pressure and resistance development over time for the experiment using the cross-linked flocculant (CR 1) and the crossflow velocity of $0.4\,\mathrm{L/min}$. Figure B.3 shows the pressure and resistance development over time for the experiment using the cross-linked flocculant (CR 2) and the crossflow velocity of $0.4\,\mathrm{L/min}$.

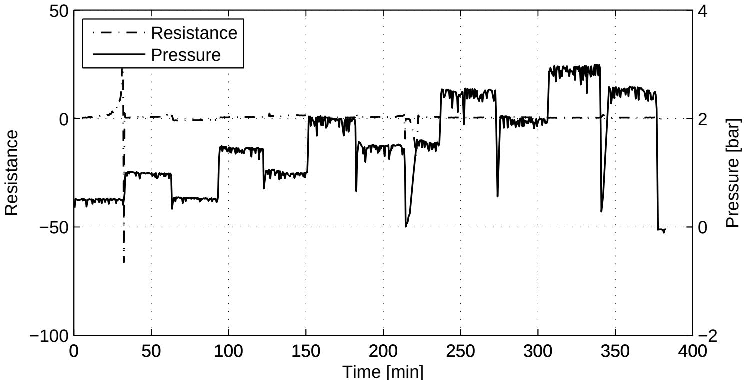

Figure B.1: Resistance development over time and the pressure over time for the filtration of the long polymer CR 0.5 and a flow of 0.4 L/min

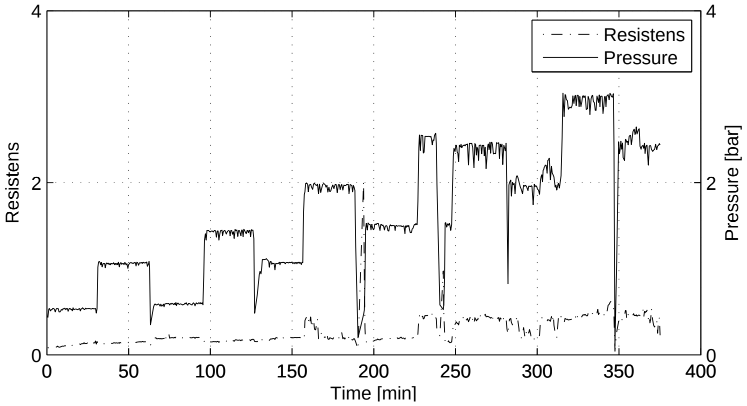

Figure B.2: Resistance development over time and the pressure over time for the filtration of the long polymer CR 1 and a flow of 0.4 L/min

B.2 Short Polymer

Figure B.4 shows the pressure and resistance development over time for the experiment using the short flocculant (CR 0.5) and the crossflow velocity of 0.4 L/min . Figure B.5 shows the pressure and resistance development over time for the experiment using the short flocculant (CR 1) and the crossflow velocity of 0.4 L/min . Figure B.6shows the pressure and resistance development over time for the experiment using the short flocculant (CR 2) and the crossflow velocity of 0.4 L/min .

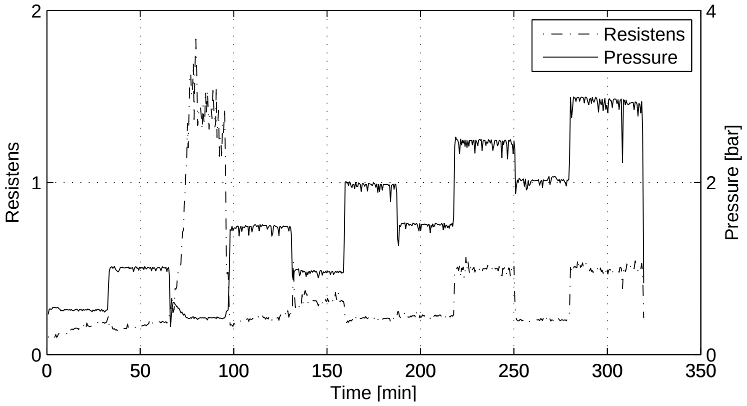

Figure B.3: Resistance development over time and the pressure over time for the filtration of the long polymer CR 2 and a flow of 0.4 L/min

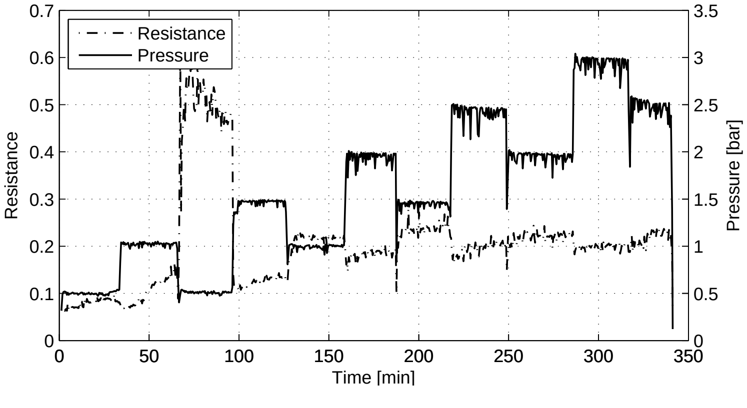

Figure B.4: Resistance development over time and the pressure over time for the filtration of the long polymer CR 0.5 and a flow of 0.6 L/min

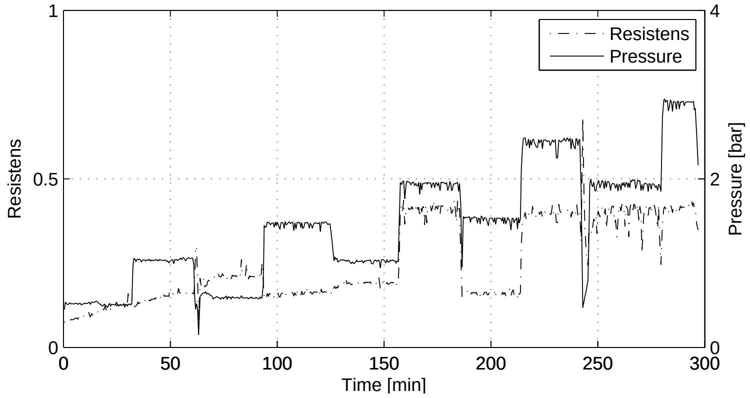

Figure B.5: Resistance development over time and the pressure over time for the filtration of the long polymer CR 1 and a flow of 0.4 L/min

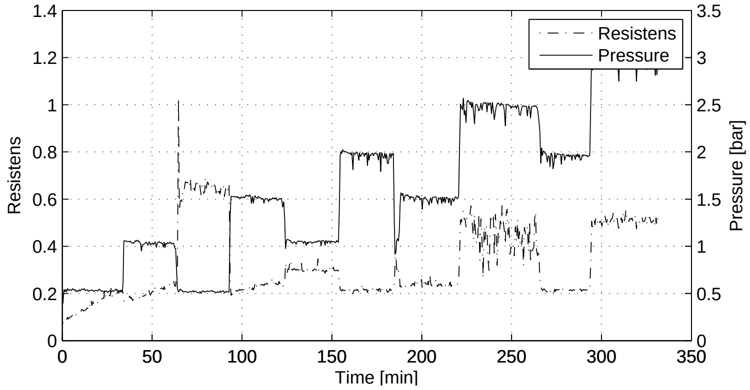

Figure B.6: Resistance development over time and the pressure over time for the filtration of the long polymer CR 2 and a flow of 0.4 L/min